A conserved motif in human BTG1 and BTG2 proteins mediates interaction with the poly(A) binding protein PABPC1 to stimulate mRNA deadenylation

Hamza Amine, Nina Ripin, Sahil Sharma, Georg Stoecklin, Frédéric Allain, Bertrand Séraphin, Fabienne Mauxion

A conserved motif in human BTG1 and BTG2 proteins mediates interaction with the poly(A) binding protein PABPC1 to stimulate mRNA deadenylation

Hamza Amine[1-4](ORCID 0000-0001-9811-1283), Nina Ripin[5, #](ORCID 0000-0001-6099-6506), Sahil Sharma[6, §](ORCID 0000-0003-4067-5419), Georg Stoecklin[6](ORCID 0000-0001-9284-9834), Frédéric H Allain[5, 7](ORCID 0000-0002-2131-6237), Bertrand Séraphin[1-4,*](ORCID 0000-0002-5168-1921) and Fabienne Mauxion[1-4,*] (ORCID 0000-0003-0554-8211)

1 Institut de Génétique et de Biologie Moléculaire et Cellulaire (IGBMC), Illkirch, France

2 Centre National de Recherche Scientifique (CNRS) UMR 7104, Illkirch, France

3 Institut National de Santé et de Recherche Médicale (INSERM) U1258, Illkirch, France

4 Université de Strasbourg, Illkirch, France

5 Department of Biology, Institute of Molecular Biology and Biophysics, ETH Zürich, Switzerland

6 Mannheim Institute for Innate Immunoscience (MI3), Medical Faculty Mannheim, Heidelberg University, Mannheim, Germany, and Center for Molecular Biology of Heidelberg University (ZMBH), German Cancer Research Center (DKFZ)-ZMBH Alliance, Heidelberg, Germany

7 Department of Biology, Institute of Biochemistry, ETH Zürich, Switzerland

* Correspondence should be addressed to BS (seraphin@igbmc.fr) or FM (mauxion@igbmc.fr)

#: present address: Department of Chemistry and Biochemistry, University of Colorado, Boulder, CO, USA

§: present address: Institute of Molecular Infection Biology (IMIB), University of Würzburg, Germany

ABSTRACT

Antiproliferative BTG/Tob proteins interact directly with the CAF1 deadenylase subunit of the CCR4-NOT complex. This binding requires the presence of two conserved motifs, boxA and boxB, characteristic of the BTG/Tob APRO domain. Consistently, these proteins were shown to stimulate mRNA deadenylation and decay in several instances. Two members of the family, BTG1 and BTG2, were reported further to associate with the protein arginine methyltransferase PRMT1 through a motif, boxC, conserved only in this subset of proteins. We recently demonstrated that BTG1 and BTG2 also contact the first RRM domain of the cytoplasmic poly(A) binding protein PABPC1. To decipher the mode of interaction of BTG1 and BTG2 with partners, we performed nuclear magnetic resonance experiments as well as mutational and biochemical analyses. Our data demonstrate that, in the context of an APRO domain, the boxC motif is necessary and sufficient to allow interaction with PABPC1 but, unexpectedly, that it is not required for BTG2 association with PRMT1. We show further that the presence of a boxC motif in an APRO domain endows it with the ability to stimulate deadenylation *in cellulo* and *in vitro*. Overall, our results identify the molecular interface allowing BTG1 and BTG2 to activate deadenylation, a process recently shown to be necessary for maintaining T-cell quiescence.

Keywords: RNA decay, CCR4-NOT complex, deadenylase, regulation of gene expression, APRO domain, poly(A) tail, poly(A) binding protein PABPC, protein arginine methylase PRMT1, antiproliferative activity, cancer

INTRODUCTION

Members of the BTG/Tob family of proteins (BTG for B-cell translocation gene and Tob for Transducer of ErbB2) are characterized by the presence of a conserved domain at their N-terminus, the BTG domain, also called the APRO domain [1]. These proteins are present in metazoans, with 6 members in vertebrates. The latter can be classified in three subgroups based on their overall organization and sequence similarity (Fig. 1): the two closely related factors with short C-terminal tails BTG1 and BTG2, the two related Tob1 and Tob2 proteins possessing the longest C-terminal moiety, and the more distantly related BTG3 and BTG4 proteins [1-3]. In addition to a common organization, BTG1 and BTG2 present at the C-terminus of their BTG/APRO domains a boxC motif [4], hereafter defined as the 11 amino-acid long sequence DGSICVLYEAS in BTG1 and DGSICVLYEEA in BTG2. Besides sequence similarities, the BTG/Tob proteins have been associated with anti-proliferative properties as their ectopic over-expression in cultured cells reduces cell proliferation [5-12]. Consistently, their endogenous expression was often observed to correlate with cell cycle arrest [13-17]. Moreover, numerous analyses have reported their connection to human cancers and suggested tumor suppressor functions (reviewed in [3, 18, 19]). In particular, correlations between their level of expression, disease progression and survival outcome have been observed and, on this basis, they were proposed as candidate prognosis biomarkers [20-22]. BTG/Tob proteins are also involved in cellular differentiation. In particular, BTG1 and BTG2 have been implicated in neuronal development (reviewed in [23]) and hematopoiesis [16, 17, 19, 24, 25].

Remarkably, several BTG/Tob proteins were independently found to interact with CAF1 [9, 26, 27]. The latter is a subunit of the CCR4-NOT complex, a multi-protein assembly conserved in all eukaryotes that was shown to be the predominant deadenylase catalyzing the mRNA poly(A) tail shortening that initiates eukaryotic mRNA decay ([28-33] to cite a few). Two subunits of the CCR4-NOT complex harbor deadenylase activities, CAF1, for which 2

paralogues named CNOT7 and CNOT8 exist in mammals, and CCR4, with 2 paralogues in mammals as well: CNOT6 and CNOT6L. BTG/Tob proteins directly bind to either the CNOT7 or the CNOT8 deadenylase (those will collectively be referred to as CAF1). This interaction has been documented at the structural level through the resolution of the crystal structure of a complex containing human CNOT7 and a N-terminal part of human Tob1 [34]. This showed that the Tob1-CAF1 interaction involves residues of the strongly conserved boxA and boxB motifs found within the globular fold of the APRO domains, supporting the idea that all BTG/Tob proteins adopt a similar mode of interaction with CAF1 and that their evolutionary conserved role is to impact the functions of the CCR4-NOT complex. The resolution of the structures of free human and mouse BTG2 revealed that its 3D organization is similar to the one of the N-terminal region of Tob1 [35]. In the BTG2 structure, boxC corresponds essentially to the final beta-strand of the APRO domain [35]. Overall, structural analyses established that the APRO domain folds as a unique and independent globular module, which does not significantly change its conformation upon CAF1 binding.

Functionally, ectopic over-expression of BTG2 or Tob1 in cells stimulated CAF1 activity leading to deadenylation and decay of RNA reporters and endogenous transcripts [36-38]. Importantly, the ability of the BTG/Tob proteins to stimulate mRNA deadenylation and decay correlated with their anti-proliferative activity [11, 12, 39]. In contrast to BTG proteins, Tob factors present in their C-terminal regions two PAM2 motifs (Poly(A)-Binding-Protein-Interacting Motif 2) that mediate their association with the MLLE domain of cytoplasmic Poly(A)-Binding-Proteins (PABPC) [40-42]. Mutations in PAM2 motifs that abrogate Tob1 binding to PABPC also abrogated Tob1 capacity to stimulate mRNA deadenylation [36, 37]. These observations suggested a model by which Tob proteins stimulate RNA deadenylation by recruiting the CCR4-NOT complex to mRNA through their interaction with PABPC. This hypothesis was further supported by tethering experiments: when Tob proteins were bound

directly to transcript reporters via tethering, their ability to stimulate deadenylation of the reporter didn't depend anymore on intact PAM2 motifs [39]. Unexpectedly, BTG1 and BTG2 were also found to interact directly with PABPC1 [12]. This observation suggested that BTG1 and BTG2 use a mechanism similar to Tob factors to stimulate mRNA deadenylation, even though the motifs involved in the respective interactions of these proteins with PABPC differ. Consistently, in the absence of PAM2 motifs in BTG1 and BTG2 factors, a mutational analysis revealed that a 4 amino acid substitution in the boxC motif, a region conserved in the APRO domain of BTG1 and BTG2 but absent from Tob factors, BTG3 and BTG4, blocked BTG2 binding to PABPC1 and its ability to stimulate deadenylation [12].

Based on yeast 2-hybrid assay results, the protein arginine methyltransferase PRMT1 was reported to interact with BTG1 and BTG2, but not with BTG3 [4, 43]. Deletion mapping suggested that the boxC motif was required for PRMT1 interaction with BTG1 and BTG2 [4]. Following this initial analysis, expression of BTG1 or BTG2 proteins containing or lacking their boxC motif was used to interpret their biological impacts as being mediated by PRMT1, for example during erythrocyte differentiation [24], following stimulation of B lymphoma cells [44] or for induction of cell-cycle arrest of pre-B cells [16].

The observations that mutation or deletion of the BTG1/2 boxC motif impaired binding to PABPC1 or PRMT1, respectively, raised the need to better understand the role of this motif in mediating interaction with partners. Here, we confirm that BTG1 and BTG2 boxC is the principal site mediating interaction of their APRO domains with PABPC1. We show further that, when grafted into another APRO domain, this sequence is sufficient to promote interaction with PABPC1. In contrast, we were unable to corroborate that the boxC motif is directly involved in the BTG2-PRMT1 interaction. Thus, our results reveal that the biological effects attributed to the recruitment of PRMT1 by BTG1 and BTG2, based on their obliteration in boxC deletion mutants, should be carefully reinterpreted. Indeed, our results

indicate that BTG1 and BTG2 boxC is a key determinant for their capacity to induce general deadenylation. This process was shown to contribute to various biological programs such as the maintenance of T cells in a quiescent state [17, 45].

MATERIAL AND METHODS

Plasmid constructions

Plasmids and oligonucleotides used in this study are presented in Supplementary Table 1 and 2, respectively. DNA fragments amplified with PCR were verified by sequencing.

Cell culture and transfections

HEK293 cells stably expressing CNOT7-TAP fusion protein [46], and HEK293 Tet-Off cells [38], were maintained in DMEM medium containing 4.5 g/l glucose, GlutaMAX, 10% fetal calf serum and 40 µg/ml gentamycine. They were transfected with TurboFect transfection reagent (Thermo Scientific) according to the manufacturer's recommendation.

RNA extraction and RACE-PAT

Total RNA was extracted using the NucleoSpin RNA kit (Macherey-Nagel). To monitor the poly(A) tail length of the β-globin transcript reporter, a modified RACE-PAT assay was performed as described previously [12, 46]. PCR products were fractionated on 3% agarose gels, stained with ethidium bromide. Those were digitized using Typhoon FLA 9500 (GE Healthcare) and quantification was done using the ImageJ software [47].

Protein co-immunoprecipitation and western blot

Co-immunoprecipitation experiments were performed using GFP-Trap magnetic agarose beads (Chromotek). Specifically, cells grown in 10cm dishes were lysed 24 hours after transfection in 200µl lysis buffer (10 mM Tris-HCl pH 8.0, 150 mM NaCl, 0.5mM EDTA, 0.5% Igepal CA-630) supplemented with protease inhibitors (Complete Protease Inhibitor Cocktail EDTA-free, Roche). After centrifugation, 300 µl of wash buffer (10 mM Tris-HCl pH 7.5, 150 mM NaCl and 0.5 mM EDTA) was added to the supernatant. Cell lysates were then incubated with 10 µl GFP-Trap magnetic beads for 1 hour at 4 °C. After recovery, beads were washed three times with wash buffer and eluted 10 min at 95°C with Laemmli sample

buffer (60 mM Tris-HCl pH 6.8, 10% glycerol, 0.002% bromophenol blue, 2% sodium dodecyl sulfate and 5% dithiothreitol).

Western blotting was performed by standard procedures and visualized with the Amersham Imager 600 (GE Healthcare). CNOT7-TAP, GFP fusion proteins and PRMT1 were revealed with peroxidase anti-peroxidase soluble complex (P1291, Sigma-Aldrich) used at 1/3000 dilution, monoclonal antibody anti-GFP (JL-8, Clontech) used at 1/2000 dilution and monoclonal antibody anti-PRMT1 (PRMT1-171, Sigma-Aldrich) used at 1/1000 dilution respectively. The Luminata Crescendo Western HRP Substrate (Millipore) was used as HRP substrate.

Yeast two-hybrid assay

The diploid yeast strain Y187/L40 (*MATα/MATa, ade2-101/ade2, his3-200/his3Δ200, leu2-3,-112/leu2-3,-112, lys2-801am::LYS2::(lexAop)4-HIS3/LYS2, MEL1/?, met-/MET, trp1-901/trp1-901, gal4Δ/gal4-542, gal80Δ/gal80-538, ura3-52::URA3::GAL1UAS-GAL1TATA-lacZ/URA3::(lexAop)8-lacZ*) was transformed simultaneously with the LexA-Binding-Domain and Gal4-Activating-Domain-derived plasmids by standard LiAc procedure. Interaction between the different chimeric proteins was monitored by β-galactosidase production using the Beta-Glo Assay System (Promega) according to the manufacturer's recommendation.

Purification of recombinant proteins

Recombinant proteins were produced in *E. coli* BL21-CodonPlus strain (Stratagene) grown in autoinduction media (Formedium).

GST and GST-BTG2(APRO). Bacteria were lysed by sonication in buffer (30 mM HEPES-KOH pH 7.5, 100 mM NaCl, 1 mM CHAPS and 2 mM dithiothreitol (DTT)) supplemented with protease inhibitors (Complete Protease Inhibitor Cocktail EDTA-free, Roche) and Benzonase (BaseMuncher, Expedeon). GST-tagged proteins were purified with affinity

chromatography on GSTrap FF column and then on Sephacryl S200 16/50 column (GE Healthcare Life Sciences) with PBS 1X and stored in PBS 1X.

6His-PABPC1(1–190) and 6His-CNOT7: Bacteria were resuspended in lysis buffer (30 mM HEPES-KOH pH 7.5, 300 mM NaCl and 1 mM DTT) supplemented with protease inhibitors (Complete Protease Inhibitor Cocktail EDTA-free, Roche) and Benzonase (BaseMuncher, Expedeon) and lysed by sonication. Proteins were purified with affinity chromatography on HisTrap FF crude column (GE Healthcare Life Sciences) followed by a size exclusion chromatography step on Superdex 75 column (GE Healthcare Life Sciences). Proteins were stored in gel filtration buffer containing 20 mM HEPES-KOH pH 7.5, 50 mM NaCl and 0.5 mM TCEP. 6His-CNOT7 sometime appeared as a doublet probably owing to trimming a few N- or C-terminal unstructured and less conserved residues with this construct [34].

GST-Tob1(APRO) and GST-Tob1-DGSICVLYEEA. Bacteria were lysed by sonication in buffer (50 mM Tris-HCl pH 8, 150 mM NaCl and 2 mM dithiothreitol (DTT)) supplemented with protease inhibitors (Complete Protease Inhibitor Cocktail EDTA-free, Roche). GST-tagged proteins were purified with affinity chromatography on GSTrap FF column and then on Sephacryl S200 16/50 column (GE Healthcare Life Sciences) with PBS 1X and stored in PBS 1X.

Recombinant proteins for NMR studies. Recombinant 6His-PABPC1 RRM2 (amino acids 85 to 190) and 6His-GB1-fusion proteins (PABPC1 RRM1, amino acids 1 to 99, BTG2 and BTG2(APRO), amino acids 1 to 126) were over expressed in BL21(DE3) Codon plus (RIL) cells (Novagen). Cells were grown in LB rich or M9 minimal media supplemented with $^{15}NH_4Cl$ or $^{15}NH_4Cl$ and ^{13}C-glucose at 37°C until OD_{600} reached 0.6-0.8, then protein expression was induced with 0.5 mM isopropyl β-D-thiogalactoside (IPTG) at 20°C for 19 to 22 hours. Cells were harvested at 4°C, 20 min at 6000rpm and pellets were lysed with a microfluidizer at 75 PSI (0.52 MPa) in 20 mM Tris-HCl pH 8, 800 mM NaCl, 2 mM $MgSO_4$,

5 mM $CaCl_2$, 10 mM imidazole, 10 mM β-mercaptoethanol, 0.25 mg/mL lysozyme, 10 µg/mL DNase, one complete EDTA free protease inhibitor tablet (Roche) in a total volume of 50 mL. Lysate cleared by centrifugation at 4°C for 30 min at 17000 rpm was applied onto a 5 ml HiTrap Chelating HP column (GE Healthcare) charged with nickel on an AKTA prime system, washed with 20mM Tris-HCl pH 8, 800 mM NaCl, 10 mM imidazole and 10 mM β-mercaptoethanol and eluted with 50% of the same buffer but containing 500 mM imidazole. Pooled fractions were dialyzed against 3 L buffer (20 mM Na_2HPO_4 pH 7, 100 mM NaCl, 1 mM EDTA, 1 mM DTT) in the presence of an in house made TEV protease (1:50 ratio mg-TEV: mg-purified protein) at RT overnight to remove the 6His-GB1-tag. Additional dialysis against 2 L of the same buffer but without EDTA was performed for 4 hours. The protein was further purified by reloading the sample on the HiTrap Chelating HP column to remove the 6His-GB1-tag, overnight dialyzed as above, followed by size exclusion chromatography using the Superdex75 prep grade size exclusion column (GE Healthcare) in 20 mM Na_2HPO_4 pH 7, 100mM NaCl, 1mM DTT. 6His-PABPC1-RRM2 was purified as above but without the TEV cleavage and the second HiTrap Chelating HP column step. The proteins were stored at -80°C.

NMR spectroscopy

Backbone experiments were performed in 20 mM MES pH 5.5, 50 mM NaCl, 1 mM DTT, 10% D_2O, 298K for PABPC1 RRM1 and in 20 mM Na_2HPO_4 pH 7, 100 mM NaCl, 1 mM DTT, 298K for BTG2(APRO) at 600 MHz. For the ^{1}H, ^{15}N and ^{13}C assignments of the protein backbone of PABPC1 RRM1 and BTG2(APRO), 2D ^{1}H,^{15}N-HSQC and 3D HNCO, HN(CA)CO, HNCA, HN(CO)CA, HNCACB, CBCA(CO)NH and 3D 15N-NOESY-HSQC (mixing time of 100 ms) spectra were recorded.

NMR titrations were done in 20 mM Na_2HPO_4 pH 7, 100 mM NaCl,1 mM DTT, 10% D_2O at 298K using Bruker AVIII-500 MHz, AVIII-600 MHz and AVIII-700 MHz (equipped with

cryoprobes). As the backbone experiments of RRM1 were recorded in a different buffer, an additional 3D HNCACB of PABPC1 RRM1 validated the backbone assignments also in the phosphate buffer. For titration experiments, unlabeled proteins were titrated into ^{15}N labelled proteins at 100-400 μM. The combined chemical shift difference was calculated according to $(\delta H^2+(\delta N/6.51)^2)^{1/2}$, were δH and δN were the difference in the ^{1}H and ^{15}N chemical shifts respectively. NMR data were processed with Topspin 3.1 (Bruker) and the analysis performed using Sparky (T. D. Goddard and D. G. Kneller, SPARKY 3, University of California San Francisco). The backbone assignments of PABPC1 RRM1 and BTG2(APRO) have been deposited in the BMRB data bank under Accession Number 50526.

In vitro deadenylation assays

In vitro deadenylation assays were performed in 60 μL final reaction volume using 100 nM of a synthetic 20(A) RNA oligonucleotide labelled with Fluorescein at its 5′ end (Dharmacon), 0.7 μM of 6His-PABPC1(1–190), 1.8 μM of GST, GST-BTG2(APRO), GST-Tob1(APRO) or GST-Tob1-DGSICVLYEEA fusion proteins, and 0.4 μM of 6His-CNOT7. Reactions were performed at 30°C in buffer containing 20 mM HEPES-KOH pH 8.0; 100 mM KCl; 0.5 mM DTT; 0.1% Igepal CA-630; 5 mM MgAc. At indicated time points, one aliquot (10 μL) of the reaction was mixed with an equal volume of RNA dye buffer (100 mM Tris-HCl pH 7.5; 1 mM EDTA; 0.001% bromophenol blue; 0.001% xylene cyanol; 0.05% sodium dodecyl sulfate; and 92% formamide) and kept on ice. Products were fractionated by electrophoresis on 15% denaturing polyacrylamide gel, detected with a Typhoon FLA 9500 (GE Healthcare), and quantified with the ImageJ software.

RESULTS

NMR mapping of residues mediating the BTG2-PABPC1 interaction strengthens the key role of the boxC motif

We previously reported that BTG1 and BTG2 APRO domains interact with the first RRM domain of the cytoplasmic Poly(A)-Binding Protein PABPC1 [12]. Furthermore, a 4 amino acid substitution in BTG2 boxC specifically impaired binding with PABPC1 RRM1 [12]. Yet, as the structure of the BTG2 APRO - PABPC1 RRM1 heterodimer remains unknown, one couldn't exclude that the boxC mutation indirectly affected association of these two factors without targeting directly the interaction interface. To identify residues involved in protein contact between BTG2 and the RRM1 domain of PABPC1, we resorted to NMR chemical shift mapping. We carried out backbone resonance assignments of BTG2(APRO) and titrations of recombinantly expressed ^{15}N labelled BTG2(APRO) and unlabeled PABPC1 RRM1, or RRM2 as a control, monitoring resonances in ^{1}H-^{15}N-HSQC spectra (Fig. 2 and Supplementary Fig. 1). The chemical shift perturbations of ^{15}N labelled BTG2(APRO) upon PABPC1 RRM1 addition are mostly in intermediate to fast exchange regime on the NMR time scale (Fig. 2A and B). In contrast, upon RRM2 addition, only a few chemical shifts show fast exchange regime, indicating a very weak or unspecific binding of BTG2(APRO) to PABPC1 RRM2 (Fig. 2B blue and Supplementary Fig. 1). These data confirm the specificity of the BTG2 APRO-PABPC1 RRM1 interaction. In these spectra, 73% of the BTG2(APRO) backbone residues are assigned, others being absent most likely because some exchanges cause line broadening and/or because of multiple conformation. Nevertheless, all central β-strands of the known human BTG2 structure (pdb code 3DJU, [35], Fig. 2C) could be assigned. Mapping residues whose chemical shift perturbations disappear at a ratio of BTG2(APRO)-RRM1 above 1:0.25/1:0.5 and those with large chemical shift perturbations (twice above the standard deviation) on the protein sequence and on the 3D-structure identifies a region of

BTG2 that is likely to mediate the interaction with PABPC1 RRM1 (Fig. 2B and 2C). Interestingly this region encompasses the boxC motif as well as the contiguous C-terminal region of boxB and adjacent amino acids in the folded protein (notably at the C terminus of the first α-helix). Most importantly, it contains the residues whose substitution was previously reported to block interaction with PABPC1 RRM1 [12]. Specificity was demonstrated by the fact that chemical shifts were not observed anymore when the ^{15}N labelled mutant BTG2(APRO) domain carrying the 4 amino-acid substitution (BTG2-kGpvkVLYEEA, residues substituted in boxC are in lowercase) was mixed with unlabeled PABPC1 RRM1 (Fig. 2D).

In converse experiments, using ^{15}N labelled PABPC1 RRM1 and unlabeled BTG2, we mapped PABPC1 residues whose chemical shifts are altered upon binding. Backbone resonance assignments of RRM1 revealed the involvement of RRM1 α1, β2 (Fig. 3A and B) and the loop following β2. Interestingly, residues within α1 such as T23, M26 and Y28 showed the strongest shifts and multiple residues in α1 disappeared already at a 1:0.25 RRM1:BTG2 ratio. These major changes in chemical environment indicate direct interactions or conformational modifications of this element. Consistently, these shifts were not detected when the BTG2(APRO) domain carrying the 4 amino-acid substitution (BTG2-kGpvkVLYEEA) preventing its interaction with PABPC1 RRM1 was used (Fig. 3C). Most residues whose chemical shifts are altered upon binding of BTG2 to PABPC1 form a contiguous surface on RRM1 (Fig. 3D, pdb code 1CVJ, [48]), suggesting its direct involvement in the interaction with BTG2.

Altogether, these NMR experiments confirm the involvement of BTG2 boxC and show chemical shift changes in the C-terminal end of α1 and part of the β-sheet, notably boxC residues, upon binding of PABPC1 RRM1. Conversely, PABPC1 RRM1 recognizes BTG2 via its α1, β2 and loop following β2.

BTG2 boxC motif is sufficient to mediate interaction to PABPC1

As NMR analyses confirmed a direct role of the BTG2 boxC motif in binding PABPC1, we next tested whether boxC in the context of an APRO domain, might be sufficient for this interaction. The BTG2-PABPC1 interaction was monitored through β-galactosidase production in a yeast 2-hybrid assay. We had previously used this system to show that a N-terminal region of human PABPC1 encompassing its first and part of its second RRM domains (amino acids 1 to 146) interacts with the BTG1 and BTG2 APRO domains, but not with the Tob1 APRO domain ([12], see also BTG1(APRO), BTG2(APRO) and Tob1(APRO) in Fig. 4A and B). Using the structural similarity between the APRO domains of BTG2 and Tob1 [34, 35] to guide site-directed mutagenesis experiments, we constructed BTG1, BTG2 and Tob1 derivatives where sequences corresponding to boxC were exchanged (Fig. 4A). These constructs are named according to the protein backbone (BTG2 or Tob1) followed by the sequence of the boxC region with residues DGSICVLYEEA present in BTG2 (or common to BTG2 and Tob1) in upper case and residues from Tob1 in lower case (kGpvkVLYvdd, note the 4 shared residues in upper case) (Fig. 4A). Control assays and the ^{1}H-^{15}N-HSQC spectra of BTG2(APRO) and BTG2(APRO) boxC mutant (BTG2-kGpvkVLYEEA) demonstrated that these mutations did not strongly affect the folding of the APRO domain in these derivatives as they were still able to interact with human CNOT7 (Fig. 4B) and the chemical shift changes were only observed in the corresponding boxC region and the neighboring β3 strand (Fig. 2A and D). Consistent with previous results [12], substituting 4 of the 5 residues at the N-terminus of boxC in the BTG2 APRO domain (boxC mutant construct BTG2-kGpvkVLYEEA) abolished the interaction with PABPC1(1-146) (Fig. 4B). Interestingly, introduction of a partial or complete BTG2 boxC into the Tob1 APRO domain in derivatives

Tob1-DGSICVLYvdd and Tob1-DGSICVLYEEA, respectively, was sufficient to create a binding site for the first RRM domains of PABPC1 as shown by a >10-fold increase in β-galactosidase production in the 2-hybrid assay (Fig. 4B). This gain-of-function result demonstrates the key role of boxC within the APRO domain in mediating the interaction with PABPC1. We concluded that the boxC motif in the context of an APRO fold is not only necessary but also sufficient to allow binding to the first RRM domains of PABPC1.

Grafting a boxC motif into the Tob1 APRO domain enhances its ability to stimulate deadenylation in cellulo and in vitro

Having generated Tob1 APRO domain derivatives able to bind PABPC1, we next tested whether this property also enabled the chimeric proteins to stimulate deadenylation. To this end, constructs encoding GFP- and HA-tagged wild-type BTG2 and Tob1 APRO domains, as well as their chimeric derivatives, were transfected in HEK293 Tet-Off cells [38] together with a β-globin mRNA reporter expressed under the control of a tetracycline-regulated promoter. The steady-state poly(A) tail length of the β-globin transcript was then monitored by RACE-PAT, a RT-PCR-based assay [12, 46]. In this assay, in agreement with results published previously [12], stimulation of deadenylation by the BTG2(APRO) fusion protein results in shorter poly(A) tails of the β-globin reporter as compared to control cells expressing GFP alone or the BTG2 boxC mutant (BTG2-kGpvkVLYEEA) (Fig. 5A, 5B and 5C, note that RACE-PAT was performed in duplicate to establish reproducibility). Long poly(A) tails are observed in cells expressing the wild-type Tob1 APRO domain (Fig. 5A, 5B and 5C). These tails appeared slightly longer than those detected in GFP transfected cells, probably as a result of ectopically expressed Tob1(APRO) acting as a competitor toward endogenous BTG/Tob factors, binding CAF1 without promoting deadenylation. When a partial or complete BTG2 boxC motif was grafted into the Tob1 APRO domain (Tob1-DGSICVLYvdd and Tob1-

DGSICVLYEEA), the poly(A) tails of the β-globin reporter transcript were shorter compared to those observed in cells expressing wild-type GFP-Tob1(APRO) (Fig. 5A, compare lanes 9-10 and 11-12 with lanes 7-8; profiles in Fig. 5B and box plots in Fig. 5C). Yet, expression of the Tob1 derivatives was not as efficient as expression of wild-type GFP-BTG2(APRO) in shortening the reporter poly(A) tails (Fig. 5A, compare lanes 9-12 and lanes 3-4 respectively). Since the expression level (Fig. 5D) and binding to CNOT7 (Fig. 4B) are similar between the Tob1 chimera and the BTG2(APRO) construct, we hypothesize that the Tob1 derivatives have a less potent intrinsic ability to stimulate deadenylation possibly because of reduced binding to PABPC1 relative to BTG2(APRO) (Fig. 4B). Nevertheless, this gain-of-function indicates that grafting the BTG2 boxC into a Tob1 backbone confers the ability to stimulate mRNA deadenylation *in vivo*.

To ascertain that introduction of a boxC motif in Tob1 directly enhances its ability to stimulate deadenylation, we conducted *in vitro* deadenylation assays [12] with purified CNOT7, PAPBC1and BTG/Tob derivatives. Recombinant GST-BTG2(APRO), GST-Tob1(APRO), a Tob1(APRO) derivative carrying the BTG2 boxC (GST-Tob1-DGSICVLYEEA) and GST, as well as 6His-tagged CNOT7 and 6His-tagged PABPC1(1-190) encoding its 2 first RRMs were produced in E. coli (Fig. 6A). Purified proteins were mixed with a 5'-fluorescein-labeled 20-oligoadenosine long RNA substrate and samples were collected at various time points of incubation. Monitoring the resulting deadenylation by denaturing gel electrophoresis demonstrated a progressive shortening of the oligo(A) substrate by 6His-CNOT7 in presence of 6His-PABPC1(1-190) and GST over the 60 min of the reaction (Fig. 6B, lanes 2-6). Consistent with previous results [12, 49], GST-BTG2(APRO) strongly accelerated deadenylation with 91% of the substrate completely degraded by 15 minutes (lanes 8-12). At the same time point, no completely deadenylated product was observed in the presence of GST-Tob1(APRO) (lanes 14-18). The Tob1-DGSICVLYEEA chimera accelerated deadenylation

(lanes 20-24) relative to controls, with 90% of the substrate completely deadenylated after 60 minutes (lanes 20-24). For comparison, at the same time point, only 38% of final deadenylated product was present in reactions containing wild-type Tob1(APRO) (Fig. 6B, lane 18). The enhanced ability of BTG2(APRO) to stimulate *in vitro* deadenylation relative to the recombinant Tob1 chimera parallels our *in cellulo* results (Fig. 5A, 5B and 5C). Importantly, no substrate degradation was detected when the RNA was incubated with the recombinant proteins in the absence of 6His-CNOT7 (Fig. 6B, lanes 1, 7, 13 and 19) indicating that CNOT7 was the sole activity responsible for the deadenylation observed. This result confirms that introduction of a boxC motif in the Tob1 APRO domain confers to the chimeric construct the ability to stimulate CNOT7 deadenylase activity *in vitro*.

Altogether, our results demonstrate that replacing a few residues of the Tob1 APRO domain by those of BTG2 boxC is sufficient to mediate PABPC1 binding and thereby stimulate mRNA deadenylation *in cellulo* and *in vitro*.

Association with PRMT1 is not a conserved feature of BTG/Tob proteins

It has been shown previously that BTG1 and BTG2, but not BTG3, interacted with PRMT1 in yeast 2-hybrid assays and pull-downs of *in vitro* translated proteins [4, 43]. To the best of our knowledge, there is no data documenting an interaction of Tob proteins with PRMT1. To determine which members of the human BTG/Tob protein family associate with PRMT1, we performed co-immunoprecipitation (IP) experiments with YFP-tagged full-length human BTG/Tob proteins. The proteins were expressed in HEK293 cells that stably express a TAP-tagged version of the CAF1 paralogue CNOT7 [46]. All BTG/Tob proteins co-precipitated CNOT7-TAP (Fig. 7) even though the CNOT7-TAP signal observed in the co-IP with YFP-BTG1 was reproducibly low. We have routinely observed that BTG1 co-precipitates CNOT7 less efficiently than the other BTG/Tob members even in the context of endogenous CNOT7

(Supplemental Fig. 2A). Nevertheless, YFP-BTG1 stimulated the decay of a co-expressed β-globin reporter mRNA as efficiently as BTG2 (Supplemental Fig. 2B), indicating that the YFP-BTG1 construct is functional. Assaying PRMT1 revealed efficient co-IP only with YFP-BTG2 (Fig. 7). As BTG1 has been reported to interact with PRMT1 in two-hybrid and *in vitro* binding assays [4, 43], we were surprised to observe that PRMT1 was not detected in co-precipitation with YFP-BTG1. However, given that YFP-BTG1 does not co-precipitate efficiently CNOT7, it is possible that the same applies to PRMT1. Overall, we observed that PRMT1 interacts with BTG2 but not BTG3 in co-IP experiments, consistent with the results of previous two-hybrid and *in vitro* binding assays [4, 43]. Our analysis shows further that BTG4, Tob1 and Tob2 do not co-IP PRMT1, indicating that its interaction with BTG2, and possibly BTG1, is not a general feature of all human BTG/Tob family members.

BTG2 boxC motif does not mediate the interaction of BTG2 with PRMT1

Gradual deletions from the C-terminus of BTG1 identified the boxC motif as required for its interaction with PRMT1 in a yeast 2-hybrid assay [4]. An internal boxC deletion also abolished BTG1-PRMT1 heterodimer formation. Further, in a pull-down assay, *in vitro* translated PRMT1 precipitated with GST-BTG2 but not with a boxC-deleted GST-BTG2 protein [4]. These observations led the authors to propose that the boxC motif, conserved only in the BTG1 and BTG2 APRO domains, was responsible for their association with PRMT1. As we uncovered that boxC is required for the interaction with PABPC1, we aimed to better characterize its role in mediating the association of BTG2 with PRMT1. To this end, we expressed a battery of derivatives of the BTG2 and Tob1 proteins fused to GFP and HA tags (Fig. 8A) in the HEK293 cells that stably express CNOT7-TAP, and tested their ability to co-precipitate CNOT7-TAP and endogenous PRMT1 (Fig. 8B). Deletion of the boxC motif from either the full length BTG2 protein or its APRO domain led to their inability to co-precipitate

PRMT1 (Fig. 8B). However, these constructs did not co-precipitate CNOT7-TAP either, and were furthermore poorly expressed. Moreover, GFP aggregates could be visualized in the transfected cells (Supplemental Fig. 3). We attribute these properties to improper folding of the APRO domain lacking the boxC sequence, rendering the resulting polypeptides completely inactive. Indeed, the boxC motif contributes to the globular fold of the BTG2 APRO domain as determined by X-ray crystallography [35], which likely explains the inability of boxC deletion mutants to co-precipitate CNOT7 and PRMT1. Substituting boxC residues of BTG2 by those found at equivalent positions in the structure of Tob1 (GFP-BTG2-kGpvkVLYEEA-HA and GFP-BTG2-kGpvkVLYvdd-HA) bypasses the folding problems of the mutant constructs, as shown by their ability to bind CNOT7 (Fig. 8B). These derivatives retained the ability to bind PRMT1 (Fig. 8B) revealing that the BTG2 boxC residues are not required for binding PRMT1. As some residues are conserved between the sequences of Tob1 and BTG2 (Fig. 8A), we also introduced in the BTG2 APRO domain residues found at the equivalent location in BTG3 (construct GFP-BTG2-knnafivaEEA). Notably, BTG2 boxC and its BTG3 equivalent do not share common residues. This derivative co-precipitated CNOT7, indicating that it was at least partially folded. Moreover, it also precipitated PRMT1. Taken together, these results indicate that the boxC motif is not required for the association of BTG2 with PRMT1, supporting that earlier observations were likely the result of improper folding of deletion constructs. In parallel, we also introduced the BTG2 boxC sequence in Tob1 (GFP-Tob1-DGSCIVLYvdd-HA and GFP-Tob1-DGSCIVLYEEA-HA constructs). The resulting proteins were correctly expressed, associated with CNOT7 but failed to co-precipitate PRMT1 (Fig. 8B) despite the presence of a BTG2 boxC motif. This indicates that the boxC motif is not sufficient to mediate association with PRMT1. In summary, we confirmed that the BTG2 APRO domain co-precipitates specifically with PRMT1, yet our detailed mutational analysis failed to identify a role for boxC in this association.

DISCUSSION

This study aimed to characterize the basis for binding of BTG1 and BTG2 with their PRMT1 and PABPC1 partners and the biological roles of these interactions. Our results confirm that BTG2 interacts with these two partners. While we demonstrate that its boxC motif is necessary and sufficient in the context of an APRO domain for PABPC1 binding and ensuing biological consequences, our observations indicate that, in contrast to earlier interpretations, the boxC motif is not essential for the interaction of BTG2 with PRMT1.

Evidence for the BTG1/2-PRMT1 interaction stemmed from 2-hybrid assays and pull-down of *in vitro* translated protein with recombinant factors [4, 43]. Here, we confirm the association of BTG2 with PRMT1 by co-precipitation experiments consistent with previous reports [50, 51]. We did not observe co-IP of PRMT1 with YFP-tagged BTG1 but, at this stage, cannot rule-out that this results from less efficient co-precipitation. Our data indicate further that, with the possible exception of BTG1, other BTG/Tob family members do not show interaction with PRMT1 in co-IP experiments. Original evidence for the boxC motif to be involved in the interaction of BTG1 and BTG2 with PRMT1 were based on the analysis of deletion mutants [4]. This observation is not confirmed by substitution analysis, and the discrepancy is likely due to a folding problem. Indeed, we now know that the boxC motif is an integral element of the APRO domain globular fold [34, 35]. In its absence, the entire APRO domain is likely unfolded, as indicated by its inability to bind CNOT7 (Fig. 8), and thus also incapable to bind other partners. The specific BTG2 elements needed for its association with PRMT1 remain unknown. An increase in specific protein methylation has been observed following BTG1 or BTG2 expression, and was linked to growth arrest of hematopoietic cells [16, 24, 44], inhibition of apoptosis during DNA double strand break repair [51] and regulation of transcription factor activities [50, 52, 53]. Enhanced methylation was proposed to result from the direct interaction of BTG1 and BTG2 with PRMT1, and in some instances, these effects were not observed upon

deletion of boxC from BTG1 or BTG2 [16, 24, 44]. However, in light of our observations of the impact of this mutation on the interaction with CNOT7, PRMT1 and possibly other partners, no direct mechanistic conclusions can be drawn. Identification of the elements mediating direct or indirect association of BTG2 (or BTG1) with PRMT1 will be important to decipher the mechanisms involved in these processes and in particular to verify whether increased protein methylation is a direct consequence of BTG1 or BTG2 interaction with PRMT1.

NMR structural analyses, interaction assays as well as functional analyses demonstrate that the conserved boxC motif present in BTG1 and BTG2 mediates their association with PABPC1 RRM domains. The NMR data clearly identifies boxC in BTG2 and RRM1 in PABPC1 as the two regions making direct contacts (Fig. 2 and 3). These observations agree with our interaction mapping and the fact that substitutions in boxC prevent BTG2-PABPC1 binding (Fig. 4, [12]). It is noteworthy that our results rest largely on the analyses of mutants in which residues at equivalent position to boxC were swapped between different members of the BTG/Tob family. This strategy ensured that the resulting proteins are properly folded, a conclusion supported by monitoring CNOT7 binding in addition to NMR analyses (Fig. 2 and 4).

Importantly, introduction of a boxC motif in the Tob1 APRO domain was sufficient to allow its interaction with PABPC1 and to enable stimulation of deadenylation *in cellulo* and *in vitro*. The Tob1 chimera was less efficient than BTG2(APRO) to induce poly(A) shortening in these assays, likely as a result of a lower affinity to PABPC1 (Fig. 4B) stemming from the contribution of other residues that fine tune this interaction (Fig. 2). Yet, this gain-of-function result strongly argues for a mechanism by which the BTG1 and BTG2 APRO domains recruit the CAF1 deadenylase to the 3' poly(A) extremity of mRNAs through their capacity to interact with CAF1 and PABPC1 simultaneously, thereby triggering deadenylation. In contrast, Tob proteins interact with CAF1 through their APRO domains and with PABPC1

through PAM2 motifs in their C-terminal region downstream of the APRO domain [36, 37, 39, 41]. As PAM2 motifs are also found in many other proteins involved in translational regulation and/or mRNA decay [40, 54], Tob proteins have to compete with these factors, unlike BTG1 and BTG2. The relative interactions of PAM2-containg proteins with PABPC1 depend on their differential binding affinities [55] and may be regulated by post-translational modifications [56]. Interestingly, BTG3 and BTG4 were also proposed to interact with poly(A)-binding proteins. Indeed, BTG4 has been shown to regulate, together with CAF1, maternal mRNA decay during late oocyte maturation and early embryogenesis in mice [57-59]. This agrees with the high expression of BTG4 in oocytes [57, 58]. The importance of BTG4 in these processes is emphasized by the identification of mutations in humans responsible for female infertility resulting from defects in embryonic development [60]. Yet, the mechanism by which BTG4 targets maternal mRNAs for degradation is still under debate, and may involve the association of BTG4 with the ubiquitous nuclear poly(A) binding protein PABPN1 [59], the maternally expressed PABPN1L protein [61], or the embryonic cytoplasmic poly(A) binding protein PABPC1L [58]. The latter study also reported an association between BTG3 and PABPC by co-IP experiments with ectopically over-expressed fusion proteins [58], but the consequences of these interactions are unknown. Given that BTG3 and BTG4 lack PAM2 or boxC motifs, further analyses are required to delineate their mode of interaction with poly(A)-binding proteins. Nevertheless, these observations suggest a general mode of action by which all BTG/Tob family members regulate mRNA deadenylation via a dual interaction. They serve as adaptors that recruit CAF1 deadenylases as effector enzymes, through the conserved boxA and boxB motifs of the APRO domain, to polyadenylated mRNAs via their association with poly(A)-binding proteins through a more variable mode of interaction.

As poly(A)-binding proteins cover the poly(A) tails of all cellular mRNAs, this raises the question whether BTG/Tob factors induce the deadenylation of all mRNAs or whether some

specific mRNAs are targeted. In the latter case, additional mechanisms would be required to ensure transcript specificity. Ectopic over-expression of BTG2 or Tob1 in cells has been found to target all reporters and endogenous transcripts tested [36, 38]. However, Tob1 was also shown to interact directly with the RNA-binding protein cytoplasmic polyadenylation element-binding protein 3 (CPEB3) [62], identifying a possible mechanism for preferential action. Indeed, Tob1-mediated recruitment of CAF1 to mRNAs containing CPE elements in their 3' UTR triggered their enhanced deadenylation and decay [62]. The region of Tob1 involved in the binding to CPEB3 is present downstream of its APRO domain and is conserved only in Tob1 and Tob2. Accordingly, Tob1 and Tob2 were shown to regulate the stability of the CPE-containing c-myc mRNA to control cell growth [63]. Interestingly, a recent report showed that endogenous BTG1 and BTG2 expression in naïve T cells triggers global mRNA decay [17]. This study showed further that this function is important to control naïve T cell quiescence by maintaining the activation signal below a threshold. Indeed, conditional depletion of the *Btg1* and *Btg2* genes in murine T cells led to their enhanced activation and proliferation even in the absence of stimulation [17]. These recent results confirm the important function BTG1 and BTG2 play in controlling cellular activation states by regulating global mRNA decay. The capacity of the CCR4-NOT complex to adjust the global rate of mRNA degradation [45] indicates that this is a fundamental process by which cells control gene expression patterns in organismal development and cellular differentiation programs.

FUNDING DETAILS

This work was supported by the Ligue Contre le Cancer (Equipe LabelliseÏe 2020) [to B.S.], the Agence Nationale pour la Recherche grant ANR-15-CE12-0014 [to B.S. and G.S.], ANR-10-LABX-0030-INRT performed under the programme Investissements d'Avenir ANR-10-IDEX-0002-02 and ANR-17-EURE-0023 [to B.S.], the CERBM-IGBMC, CNRS and Inserm [to F.M. and B.S.], grant STO 859/5-1 from the Deutsche Forschungsgemeinschaft [to G.S.] and the NCCR RNA and Disease [F.H.-T.A.].

ACKNOWLEDGMENTS

We acknowledge our team members for support and suggestions, and thank N. Karcher, N. Crespo and S. Bahit for assistance with plasmid construction. We also thank G. Stier and A. Geerlof [European Molecular Biology Laboratory (EMBL)] for providing the petGB1-1a plasmid.

AUTHOR CONTRIBUTIONS:

F.M. and B.S. designed the project; H.A., N.R., S.S. and F.M. performed experiments; F.M., B.S., F.H.-T.A., G.S., H.A., and N.R. analyzed the data. F.H.-T.A. supervised the NMR work. F.M., B.S., H.A., G.S., N.R., and F.H.-T.A. wrote the paper.

DISCLOSURE OF INTEREST: The authors report no conflict of interest.

REFERENCES

1. Matsuda S, Rouault J, Magaud J, Berthet C. In search of a function for the TIS21/PC3/BTG1/TOB family. FEBS Lett 2001; 497:67-72.
2. Tirone F. The gene PC3(TIS21/BTG2), prototype member of the PC3/BTG/TOB family: regulator in control of cell growth, differentiation, and DNA repair? J Cell Physiol 2001; 187:155-65.
3. Winkler GS. The mammalian anti-proliferative BTG/Tob protein family. J Cell Physiol 2010; 222:66-72.

4. Berthet C, Guehenneux F, Revol V, Samarut C, Lukaszewicz A, Dehay C, et al. Interaction of PRMT1 with BTG/TOB proteins in cell signalling: molecular analysis and functional aspects. Genes Cells 2002; 7:29-39.
5. Rouault JP, Rimokh R, Tessa C, Paranhos G, Ffrench M, Duret L, et al. BTG1, a member of a new family of antiproliferative genes. EMBO J 1992; 11:1663-70.
6. Matsuda S, Kawamura-Tsuzuku J, Ohsugi M, Yoshida M, Emi M, Nakamura Y, et al. Tob, a novel protein that interacts with p185erbB2, is associated with anti-proliferative activity. Oncogene 1996; 12:705-13.
7. Montagnoli A, Guardavaccaro D, Starace G, Tirone F. Overexpression of the nerve growth factor-inducible PC3 immediate early gene is associated with growth inhibition. Cell Growth Differ 1996; 7:1327-36.
8. Yoshida Y, Matsuda S, Ikematsu N, Kawamura-Tsuzuku J, Inazawa J, Umemori H, et al. ANA, a novel member of Tob/BTG1 family, is expressed in the ventricular zone of the developing central nervous system. Oncogene 1998; 16:2687-93.
9. Ikematsu N, Yoshida Y, Kawamura-Tsuzuku J, Ohsugi M, Onda M, Hirai M, et al. Tob2, a novel anti-proliferative Tob/BTG1 family member, associates with a component of the CCR4 transcriptional regulatory complex capable of binding cyclin-dependent kinases. Oncogene 1999; 18:7432-41.
10. Buanne P, Corrente G, Micheli L, Palena A, Lavia P, Spadafora C, et al. Cloning of PC3B, a novel member of the PC3/BTG/TOB family of growth inhibitory genes, highly expressed in the olfactory epithelium. Genomics 2000; 68:253-63.
11. Doidge R, Mittal S, Aslam A, Winkler GS. The Anti-Proliferative Activity of BTG/TOB Proteins Is Mediated via the Caf1a (CNOT7) and Caf1b (CNOT8) Deadenylase Subunits of the Ccr4-Not Complex. PLoS One 2012; 7:e51331.
12. Stupfler B, Birck C, Seraphin B, Mauxion F. BTG2 bridges PABPC1 RNA-binding domains and CAF1 deadenylase to control cell proliferation. Nature communications 2016; 7:10811.
13. Rouault JP, Falette N, Guehenneux F, Guillot C, Rimokh R, Wang Q, et al. Identification of BTG2, an antiproliferative p53-dependent component of the DNA damage cellular response pathway. Nat Genet 1996; 14:482-6.
14. Iacopetti P, Michelini M, Stuckmann I, Oback B, Aaku-Saraste E, Huttner WB. Expression of the antiproliferative gene TIS21 at the onset of neurogenesis identifies single neuroepithelial cells that switch from proliferative to neuron-generating division. Proc Natl Acad Sci U S A 1999; 96:4639-44.
15. Rodier A, Marchal-Victorion S, Rochard P, Casas F, Cassar-Malek I, Rouault JP, et al. BTG1: a triiodothyronine target involved in the myogenic influence of the hormone. Exp Cell Res 1999; 249:337-48.
16. Dolezal E, Infantino S, Drepper F, Borsig T, Singh A, Wossning T, et al. The BTG2-PRMT1 module limits pre-B cell expansion by regulating the CDK4-Cyclin-D3 complex. Nat Immunol 2017; 18:911-20.
17. Hwang SS, Lim J, Yu Z, Kong P, Sefik E, Xu H, et al. mRNA destabilization by BTG1 and BTG2 maintains T cell quiescence. Science 2020; 367:1255-60.
18. Lim IK. TIS21 (/BTG2/PC3) as a link between ageing and cancer: cell cycle regulator and endogenous cell death molecule. J Cancer Res Clin Oncol 2006; 132:417-26.
19. Yuniati L, Scheijen B, van der Meer LT, van Leeuwen FN. Tumor suppressors BTG1 and BTG2: Beyond growth control. J Cell Physiol 2019; 234:5379-89.
20. Mollerstrom E, Kovacs A, Lovgren K, Nemes S, Delle U, Danielsson A, et al. Up-regulation of cell cycle arrest protein BTG2 correlates with increased overall survival in breast cancer, as detected by immunohistochemistry using tissue microarray. BMC cancer 2010; 10:296.

21. Bai Y, Qiao L, Xie N, Shi Y, Liu N, Wang J. Expression and prognosis analyses of the Tob/BTG antiproliferative (APRO) protein family in human cancers. PLoS One 2017; 12:e0184902.
22. Shen S, Zhang R, Guo Y, Loehrer E, Wei Y, Zhu Y, et al. A multi-omic study reveals BTG2 as a reliable prognostic marker for early-stage non-small cell lung cancer. Mol Oncol 2018; 12:913-24.
23. Micheli L, Ceccarelli M, Farioli-Vecchioli S, Tirone F. Control of the Normal and Pathological Development of Neural Stem and Progenitor Cells by the PC3/Tis21/Btg2 and Btg1 Genes. J Cell Physiol 2015; 230:2881-90.
24. Bakker WJ, Blazquez-Domingo M, Kolbus A, Besooyen J, Steinlein P, Beug H, et al. FoxO3a regulates erythroid differentiation and induces BTG1, an activator of protein arginine methyl transferase 1. J Cell Biol 2004; 164:175-84.
25. Tijchon E, van Emst L, Yuniati L, van Ingen Schenau D, Havinga J, Rouault JP, et al. Tumor suppressors BTG1 and BTG2 regulate early mouse B-cell development. Haematologica 2016; 101:e272-6.
26. Bogdan JA, Adams-Burton C, Pedicord DL, Sukovich DA, Benfield PA, Corjay MH, et al. Human carbon catabolite repressor protein (CCR4)-associative factor 1: cloning, expression and characterization of its interaction with the B-cell translocation protein BTG1. Biochem J 1998; 336 (Pt 2):471-81.
27. Rouault JP, Prevot D, Berthet C, Birot AM, Billaud M, Magaud JP, et al. Interaction of BTG1 and p53-regulated BTG2 gene products with mCaf1, the murine homolog of a component of the yeast CCR4 transcriptional regulatory complex. J Biol Chem 1998; 273:22563-9.
28. Tucker M, Valencia-Sanchez MA, Staples RR, Chen J, Denis CL, Parker R. The transcription factor associated Ccr4 and Caf1 proteins are components of the major cytoplasmic mRNA deadenylase in Saccharomyces cerevisiae. Cell 2001; 104:377-86.
29. Daugeron MC, Mauxion F, Seraphin B. The yeast POP2 gene encodes a nuclease involved in mRNA deadenylation. Nucleic Acids Res 2001; 29:2448-55.
30. Temme C, Zaessinger S, Meyer S, Simonelig M, Wahle E. A complex containing the CCR4 and CAF1 proteins is involved in mRNA deadenylation in Drosophila. EMBO J 2004; 23:2862-71.
31. Wiederhold K, Passmore LA. Cytoplasmic deadenylation: regulation of mRNA fate. Biochem Soc Trans 2010; 38:1531-6.
32. Yi H, Park J, Ha M, Lim J, Chang H, Kim VN. PABP Cooperates with the CCR4-NOT Complex to Promote mRNA Deadenylation and Block Precocious Decay. Mol Cell 2018; 70:1081-8 e5.
33. Raisch T, Chang CT, Levdansky Y, Muthukumar S, Raunser S, Valkov E. Reconstitution of recombinant human CCR4-NOT reveals molecular insights into regulated deadenylation. Nat Commun 2019; 10:3173.
34. Horiuchi M, Takeuchi K, Noda N, Muroya N, Suzuki T, Nakamura T, et al. Structural basis for the antiproliferative activity of the Tob-hCaf1 complex. J Biol Chem 2009; 284:13244-55.
35. Yang X, Morita M, Wang H, Suzuki T, Yang W, Luo Y, et al. Crystal structures of human BTG2 and mouse TIS21 involved in suppression of CAF1 deadenylase activity. Nucleic Acids Res 2008; 36:6872-81.
36. Ezzeddine N, Chang TC, Zhu W, Yamashita A, Chen CY, Zhong Z, et al. Human TOB, an antiproliferative transcription factor, is a poly(A)-binding protein-dependent positive regulator of cytoplasmic mRNA deadenylation. Mol Cell Biol 2007; 27:7791-801.

37. Funakoshi Y, Doi Y, Hosoda N, Uchida N, Osawa M, Shimada I, et al. Mechanism of mRNA deadenylation: evidence for a molecular interplay between translation termination factor eRF3 and mRNA deadenylases. Genes Dev 2007; 21:3135-48.
38. Mauxion F, Faux C, Seraphin B. The BTG2 protein is a general activator of mRNA deadenylation. EMBO J 2008; 27:1039-48.
39. Ezzeddine N, Chen CY, Shyu AB. Evidence providing new insights into TOB-promoted deadenylation and supporting a link between TOB's deadenylation-enhancing and antiproliferative activities. Mol Cell Biol 2012; 32:1089-98.
40. Albrecht M, Lengauer T. Survey on the PABC recognition motif PAM2. Biochem Biophys Res Commun 2004; 316:129-38.
41. Okochi K, Suzuki T, Inoue J, Matsuda S, Yamamoto T. Interaction of anti-proliferative protein Tob with poly(A)-binding protein and inducible poly(A)-binding protein: implication of Tob in translational control. Genes Cells 2005; 10:151-63.
42. Kozlov G, Menade M, Rosenauer A, Nguyen L, Gehring K. Molecular determinants of PAM2 recognition by the MLLE domain of poly(A)-binding protein. J Mol Biol 2010; 397:397-407.
43. Lin WJ, Gary JD, Yang MC, Clarke S, Herschman HR. The mammalian immediate-early TIS21 protein and the leukemia-associated BTG1 protein interact with a protein-arginine N-methyltransferase. J Biol Chem 1996; 271:15034-44.
44. Hata K, Nishijima K, Mizuguchi J. Role for Btg1 and Btg2 in growth arrest of WEHI-231 cells through arginine methylation following membrane immunoglobulin engagement. Exp Cell Res 2007; 313:2356-66.
45. Sharma S, Poetz F, Bruer M, Ly-Hartig TB, Schott J, Seraphin B, et al. Acetylation-Dependent Control of Global Poly(A) RNA Degradation by CBP/p300 and HDAC1/2. Molecular cell 2016; 63:927-38.
46. Mauxion F, Preve B, Seraphin B. C2ORF29/CNOT11 and CNOT10 form a new module of the CCR4-NOT complex. RNA Biol 2013; 10:267-76.
47. Schneider CA, Rasband WR, Eliceiri KW. NIH Image to ImageJ: 25 years of image analysis. Nat Methods 2012; 9:671-5.
48. Deo RC, Bonanno JB, Sonenberg N, Burley SK. Recognition of polyadenylate RNA by the poly(A)-binding protein. Cell 1999; 98:835-45.
49. Pavanello L, Hall B, Airhihen B, Winkler GS. The central region of CNOT1 and CNOT9 stimulates deadenylation by the Ccr4–Not nuclease module. Biochemical Journal 2018; 475:3437-50.
50. Passeri D, Marcucci A, Rizzo G, Billi M, Panigada M, Leonardi L, et al. Btg2 enhances retinoic acid-induced differentiation by modulating histone H4 methylation and acetylation. Mol Cell Biol 2006; 26:5023-32.
51. Choi KS, Kim JY, Lim SK, Choi YW, Kim YH, Kang SY, et al. TIS21(/BTG2/PC3) accelerates the repair of DNA double strand breaks by enhancing Mre11 methylation and blocking damage signal transfer to the Chk2(T68)-p53(S20) pathway. DNA Repair (Amst) 2012; 11:965-75.
52. van Galen JC, Kuiper RP, van Emst L, Levers M, Tijchon E, Scheijen B, et al. BTG1 regulates glucocorticoid receptor autoinduction in acute lymphoblastic leukemia. Blood 2010; 115:4810-9.
53. Yuniati L, van der Meer LT, Tijchon E, van Ingen Schenau D, van Emst L, Levers M, et al. Tumor suppressor BTG1 promotes PRMT1-mediated ATF4 function in response to cellular stress. Oncotarget 2015; 7:3128-43.
54. Tritschler F, Huntzinger E, Izaurralde E. Role of GW182 proteins and PABPC1 in the miRNA pathway: a sense of deja vu. Nat Rev Mol Cell Biol 2010; 11:379-84.

55. Ruan L, Osawa M, Hosoda N, Imai S, Machiyama A, Katada T, et al. Quantitative characterization of Tob interactions provides the thermodynamic basis for translation termination-coupled deadenylase regulation. J Biol Chem 2010; 285:27624-31.
56. Huang KL, Chadee AB, Chen CY, Zhang Y, Shyu AB. Phosphorylation at intrinsically disordered regions of PAM2 motif-containing proteins modulates their interactions with PABPC1 and influences mRNA fate. RNA 2013; 19:295-305.
57. Yu C, Ji SY, Sha QQ, Dang Y, Zhou JJ, Zhang YL, et al. BTG4 is a meiotic cell cycle-coupled maternal-zygotic-transition licensing factor in oocytes. Nat Struct Mol Biol 2016; 23:387-94.
58. Liu Y, Lu X, Shi J, Yu X, Zhang X, Zhu K, et al. BTG4 is a key regulator for maternal mRNA clearance during mouse early embryogenesis. Journal of molecular cell biology 2016; 8:366-8.
59. Pasternak M, Pfender S, Santhanam B, Schuh M. The BTG4 and CAF1 complex prevents the spontaneous activation of eggs by deadenylating maternal mRNAs. Open biology 2016; 6.
60. Zheng W, Zhou Z, Sha Q, Niu X, Sun X, Shi J, et al. Homozygous Mutations in BTG4 Cause Zygotic Cleavage Failure and Female Infertility. Am J Hum Genet 2020; 107:24-33.
61. Zhao LW, Zhu YZ, Chen H, Wu YW, Pi SB, Chen L, et al. PABPN1L mediates cytoplasmic mRNA decay as a placeholder during the maternal-to-zygotic transition. EMBO Rep 2020:e49956.
62. Hosoda N, Funakoshi Y, Hirasawa M, Yamagishi R, Asano Y, Miyagawa R, et al. Anti-proliferative protein Tob negatively regulates CPEB3 target by recruiting Caf1 deadenylase. EMBO J 2011; 30:1311-23.
63. Ogami K, Hosoda N, Funakoshi Y, Hoshino S. Antiproliferative protein Tob directly regulates c-myc proto-oncogene expression through cytoplasmic polyadenylation element-binding protein CPEB. Oncogene 2014; 33:55-64.

FIGURE LEGENDS

Figure 1 – Organization of BTG/Tob proteins

The 6 human BTG/Tob proteins are schematically presented to scale with grey box indicating the APRO domain that binds to the CAF1 deadenylase. This domain contains the conserved A and B boxes as well as, in the case of BTG1 and BTG2 the C box. The scheme also indicates the location of PAM2 motifs which are present in the C-terminal extensions of TOB1 and TOB2. The latter interact with the MLLE domain of PABPC proteins.

Figure 2 – NMR identification of the BTG2 residues involved in its interaction with PABPC1 RRM domains

A) Overlay of ^{1}H-^{15}N HSQC spectra of free BTG2(APRO) (blue) and in complex with increasing amounts of RRM1 (1:0.25 red; 1:0.5 orange; 1:1 green; 1:2 cyan; 1:5 magenta). Some key residues are indicated by a box and the close-up view shown below. The number of scans (NS) is indicated.

B) Combined chemical-shift perturbations of BTG2(APRO) upon binding to RRM1 (black) or RRM2 (blue). The secondary structure and amino acid sequence are shown at the top, the boxB region is highlighted in green and boxC in violet. The black or blue horizontal line represents the two times the s.d. of all chemical shift differences. Peaks which disappear at 1:0.25 or 1:0.5 and did not return at higher ratios are indicated by bars with >0.16 ppm (dashed line).

C) Cartoon representation of the structure of the human BTG2 APRO domain (pdb code 3DJU), corresponding to the protein sequence shown in B. Residues that show significant chemical shift changes (above the 2x sd) or disappear upon addition of RRM1 are shown in blue or red respectively. Undetectable or unassignable backbone residues are colored in orange. BoxC residues are indicated in violet.

D) Overlay of ^{1}H-^{15}N HSQC spectra of BTG-kGpvkVLYEEA (blue) and BTG-kGpvkVLYEEA in complex with RRM1 (1:2, red).

Figure 3 – NMR identification of the PABPC1 RRM1 residues involved in the interaction with BTG2

A) Overlay of ^{1}H-^{15}N HSQC spectra of free RRM1 (blue) and in complex with increasing amounts of BTG2 (1:1 red; 1:2 orange). Some key residues are indicated by a box and the close-up view shown below. In the close-up view, arrows show the direction of the chemical shift change. Aliased negative peaks in pink correspond to the amides of arginine side chains. The number of scans (NS) is 2, otherwise indicated if different.

B) The combined chemical-shift perturbations of RRM1 upon binding to BTG2 (1:2.5 ratio; blue). The secondary structure is represented at the top and the region with high chemical shift changes (in α1 and β2) is highlighted in orange. Key residues are labelled. The horizontal line represents two times the s.d. of all chemical shift differences. Peaks which disappear at 1:0.25 or 1:0.5 and did not return at higher ratios are shown by bars with >0.18 ppm (dashed line).

C) Overlay of ^{1}H-^{15}N HSQC spectra of RRM1 (blue) and RRM1 in complex with increasing amounts of BTG-kGpvkVLYEEA (1:1 red; 1:2 yellow; 1:5 green).

D**)** Cartoon representation of RRM1; modified from PABP RRM12 structure (pdb code 1CVJ). Chemical-shift perturbations upon BTG2 addition larger than 2x sd are colored in red while signals which disappear at 1:0.25/0.5 are shown in blue.

Figure 4 - The boxC motif is sufficient and necessary to allow binding to PABPC1

A) Schematic representation of human BTG1, BTG2 and Tob1 proteins and mutation introduced. The conserved boxA (A) and boxB (B) motifs, signatures for the BTG/Tob

family, are indicated. The sequences mutagenized, overlapping the 11 amino acid boxC motif specific for BTG1 and BTG2, are presented with color code: amino acids of the boxC motif are in purple while equivalent residues in Tob1 are in green. To facilitate identification of substituted positions, uppercase letters indicate residues present in BTG2 boxC while lowercases correspond to amino acids specific for Tob1.

B) Interaction of wild-type and mutant BTG1, BTG2, and Tob1 APRO domains with CNOT7 and the first part of the PABPC1 multi-RRM domain in yeast two-hybrid assay. The Y187/L40 yeast strain was co-transformed with plasmids expressing the indicated LexA-Binding-Domain and Gal4-Activating-Domain fusion proteins. Interaction between the different chimeric proteins indicated was assessed by β-galactosidase assays performed in duplicates. Activities are expressed in arbitrary units and plotted on a logarithmic scale. Three biological replicates were assayed and the corresponding standard deviation plotted as error bars.

Figure 5 - Presence of a boxC motif enhances Tob1 APRO ability to stimulate deadenylation in cellulo

A) Reverse transcription polymerase chain reaction (RT-PCR) amplification of the poly(A) tails of the β-globin reporter transcript. HEK293 Tet-Off cells were co-transfected with plasmids expressing the β-globin reporter and the different HA- and GFP-tagged BTG/Tob fusion proteins as indicated (or empty GFP expression vector). Fragments comprising ~200 bp of the 3′ UTR of the β-globin mRNA in addition to poly(A) tails were amplified using a RACE-PAT assay. Experiment was repeated twice with, in each case, two biological duplicates.

B) Profiles of the poly(A) tail lengths of the β-globin reporter. The gel presented in A was quantified using ImageJ and relative average profiles were plotted after adjusting the maximal signal intensity to 100% for each lane.

C) Poly(A) tail lengths were analyzed and presented as box plots indicating weighted mean, weighted upper and lower quartile, and weighted 5-95% distribution. Significant p values (*: $p<0,05$; ** $p<0,01$) from ANOVA tests between corresponding wild-type and mutant proteins are indicated.

D) A western blot analysis of the cell lysates corresponding to the transfections performed in A is shown.

Figure 6 - A chimeric Tob1 APRO domain with a boxC motif stimulates CNOT7 deadenylase activity in vitro

A) SDS–PAGE analysis of purified recombinant proteins used in *in vitro* deadenylation assays. One microgram of purified proteins was resolved on 12% SDS–PAGE gel stained with Coomassie blue. 6His-CNOT7 appeared as a doublet.

B) *In vitro* deadenylation assay with purified CNOT7, wild-type and mutant BTG2 and Tob1 APRO domain derivatives, and first RRM domains of PABPC1. A 5′ Fluorescein-labelled poly(A) substrate of 20 residues was incubated in defined conditions (see Methods) with purified 6His-CNOT7 and 6His-PABPC1(1-190) as well as GST alone, GST-BTG2(APRO) or GST-Tob1(APRO), or GST-Tob1-DGSICVLYEEA as indicated. Reaction products were fractionated on 15% denaturing polyacrylamide gel. Experiment was performed three times with similar results.

Figure 7 - Co-precipitation of PRMT1 with BTG2

Co-immunoprecipitation of CNOT7-TAP and endogenous PRMT1 with YFP-tagged BTG/Tob proteins. HEK293 cells expressing stably CNOT7-TAP were transfected with plasmids expressing YFP-BTG/Tob fusion proteins or only YFP as control. YFP-tagged proteins were precipitated with GFP-Trap magnetic agarose beads and the co-precipitation of endogenous PRMT1 and of CNOT7-TAP was analyzed by western blotting. The anti-GFP antibody used for western blot detection weakly cross-reacts with the protein A domain of the TAP tag, hence CNOT7-TAP is also detected (marked by an asterisk). Note that the molecular weight of YFP-BTG4 is identical to the one of CNOT7-TAP. The correct expression of YFP-BTG4 is demonstrated by the co-precipitation of CNOT7-TAP that is not observed with YFP alone. YFP-BTG4 expression is also shown in Supplementary Fig. 2A.

Figure 8 - The boxC motif is not mediating the interaction of BTG2 with PRMT1

A) Schematic representation of human BTG2, BTG3, Tob1 and their derivatives used in this experiment. The same color code is used than in Fig. 4A with in addition BTG3 in orange.

B) Co-immunoprecipitation of CNOT7-TAP and PRMT1 with BTG2/Tob proteins. HEK293 cells stably expressing CNOT7-TAP were transfected with plasmids expressing GFP-BTG/Tob-HA fusion proteins or empty GFP expression vector. Proteins were precipitated with GFP-Trap magnetic agarose beads and the co-precipitation was analyzed by western blotting. CNOT7-TAP is visible after revelation with anti-GFP antibody (marked by an asterisk) because the antibody weakly binds also to the protein A domain of the TAP tag. In this experiment, the CNOT7-TAP signal is not visible in eluates because of the shorter exposition time. A weak co-precipitation with Tob1(APRO) was detected in this experiment but wasn't reproducible.

Figure 1

Figure 1

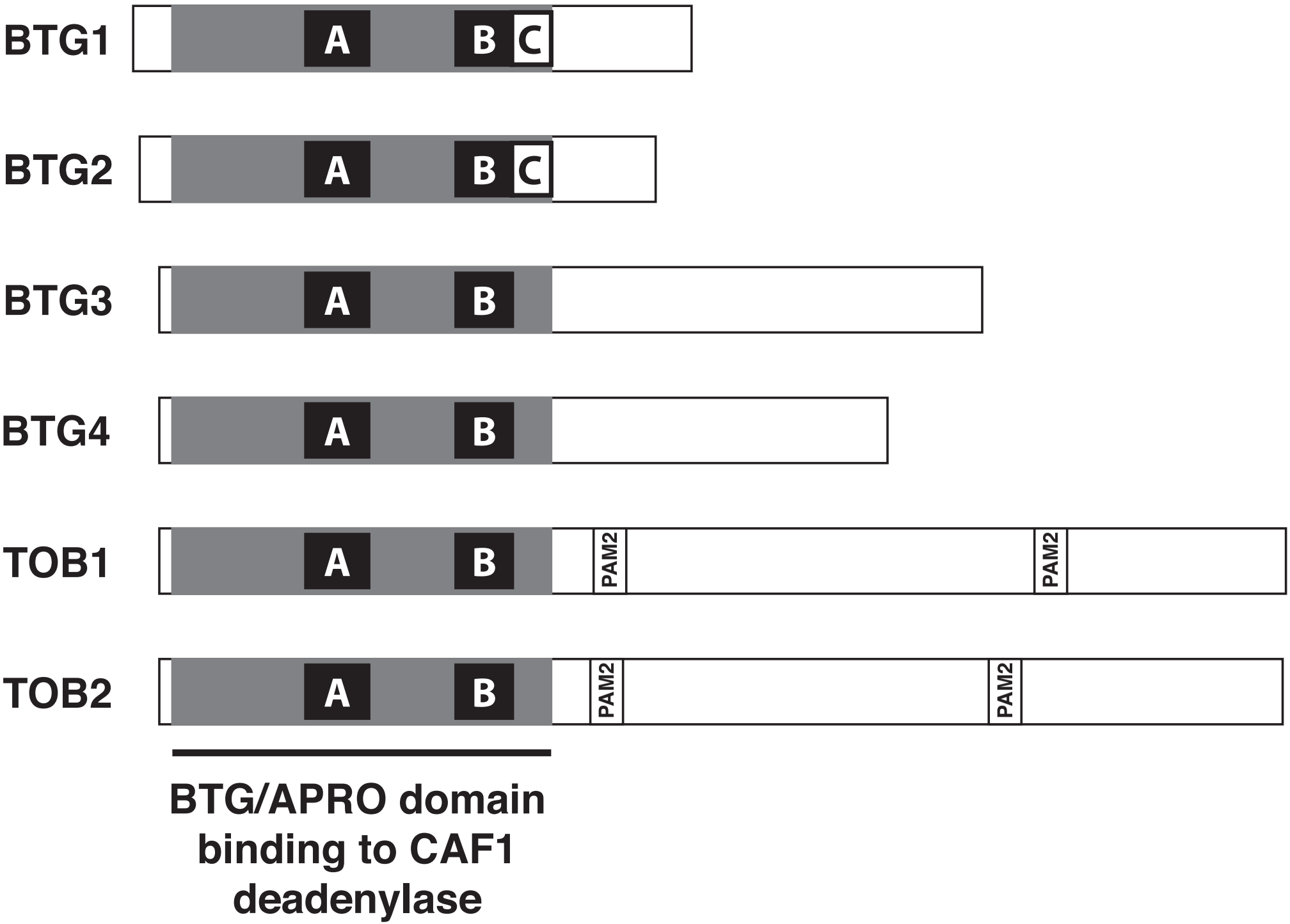

Figure 2

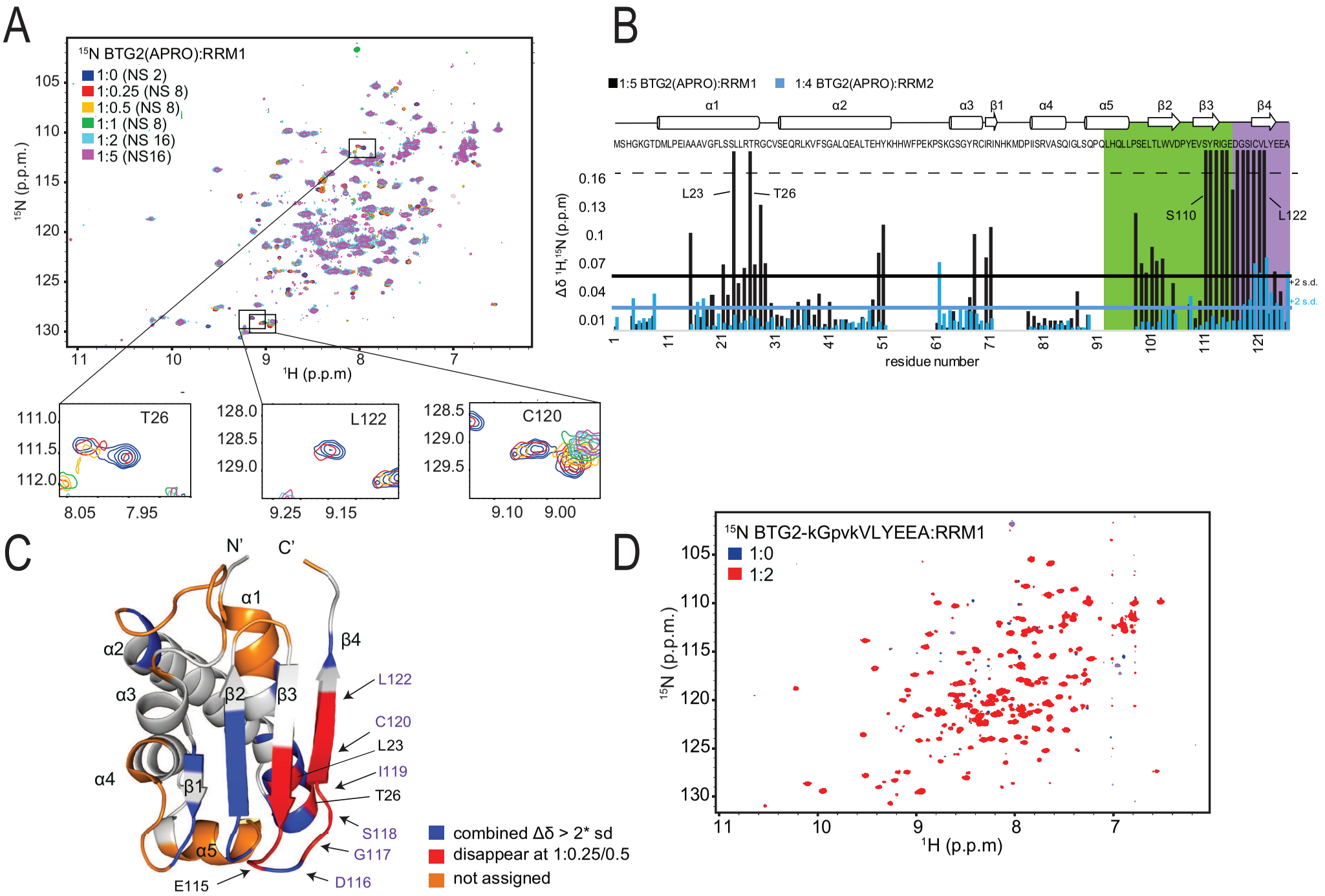
A
15N BTG2(APRO):RRM1
1:0 (NS 2)
1:0.25 (NS 8)
1:0.5 (NS 8)
1:1 (NS 8)
1:2 (NS 16)
1:5 (NS16)
15N (p.p.m.)
1H (p.p.m)
T26
L122
C120
B
1:5 BTG2(APRO):RRM1
1:4 BTG2(APRO):RRM2
α1 α2 α3 β1 α4 α5 β2 β3 β4
MSHGKGTDMLPEIAAAVGFLSSLLRTRGCVSEQRLKVFSGALQEALTEHYKHHWFPEKPSKGSGYRCIRINHKMDPIISRVASQIGLSQPQLHQLLPSELTLWVDPYEVSYRIGEDGSICVLYEEA
L23
T26
S110
L122
Δδ 1H,15N (p.p.m)
+2 s.d.
+2 s.d.
residue number
C
N'
C'
α1
α2
α3
α4
α5
β1
β2
β3
β4
L122
C120
L23
I119
T26
S118
G117
D116
E115
combined Δδ > 2* sd
disappear at 1:0.25/0.5
not assigned
D
15N BTG2-kGpvkVLYEEA:RRM1
1:0
1:2
15N (p.p.m.)
1H (p.p.m)

Figure 3

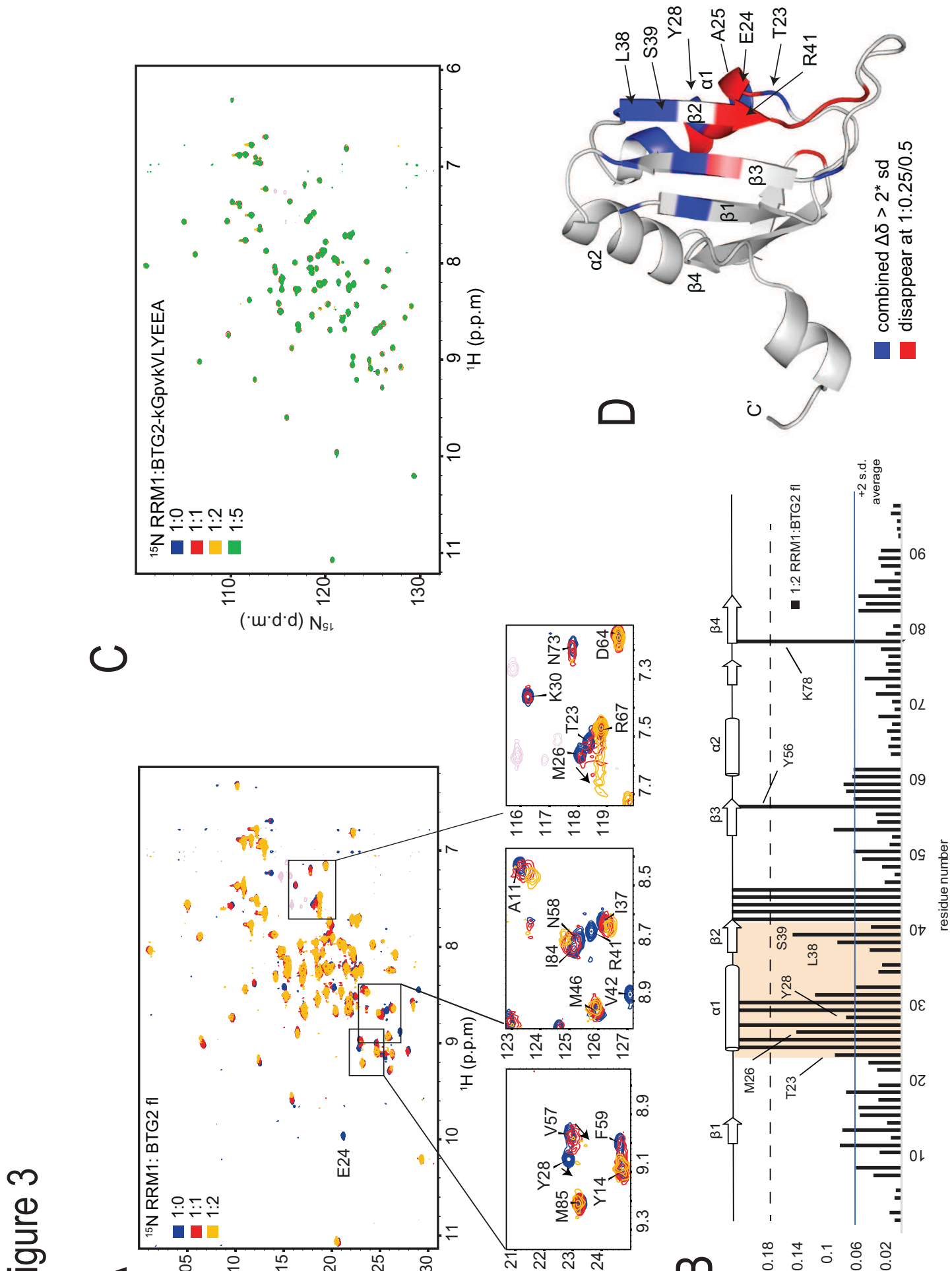
Figure 3
A
^{15}N RRM1: BTG2 fl
1:0
1:1
1:2
E24
Y28
V57
M85
Y14
F59
M26
T23
A11
N58
I84
M46
V42
R41
I37
K30
N73'
D64
R67
^{15}N (p.p.m.)
^{1}H (p.p.m)
B
β1
α1
β2
α2
β3
β4
M26
T23
Y28
S39
L38
Y56
K78
1:2 RRM1:BTG2 fl
+2 s.d. average
Δδ ^{1}H,^{15}N (p.p.m)
residue number
C
^{15}N RRM1:BTG2-kGpvkVLYEEA
1:0
1:1
1:2
1:5
^{15}N (p.p.m.)
^{1}H (p.p.m)
D
L38
S39
Y28
α1
β2
A25
E24
T23
R41
α2
β1
β3
β4
C'
combined Δδ > 2* sd
disappear at 1:0.25/0.5

Figure 4

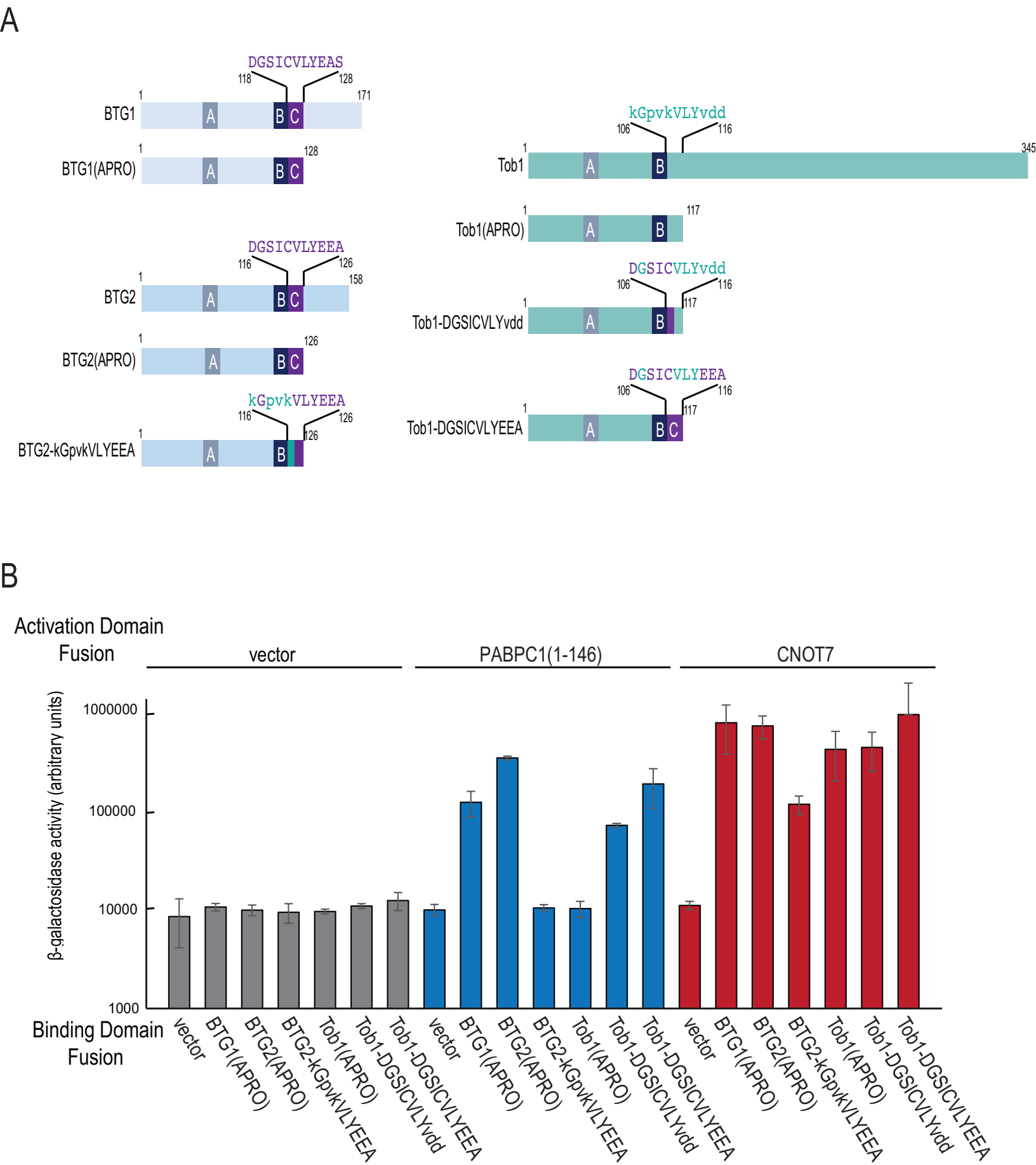
A
DGSICVLYEAS
118
128
1
171
BTG1
A
B C
1
128
BTG1(APRO)
A
B C
DGSICVLYEEA
116
126
1
158
BTG2
A
B C
1
126
BTG2(APRO)
A
B C
kGpvkVLYEEA
116
126
1
126
BTG2-kGpvkVLYEEA
A
B
kGpvkVLYvdd
106
116
1
345
Tob1
A
B
1
117
Tob1(APRO)
A
B
DGSICVLYvdd
106
116
1
117
Tob1-DGSICVLYvdd
A
B
DGSICVLYEEA
106
116
1
117
Tob1-DGSICVLYEEA
A
B C
B
Activation Domain Fusion
vector
PABPC1(1-146)
CNOT7
β-galactosidase activity (arbitrary units)
1000000
100000
10000
1000
Binding Domain Fusion
vector
BTG1(APRO)
BTG2(APRO)
BTG2-kGpvkVLYEEA
Tob1(APRO)
Tob1-DGSICVLYvdd
Tob1-DGSICVLYEEA

Figure 5

Figure 5

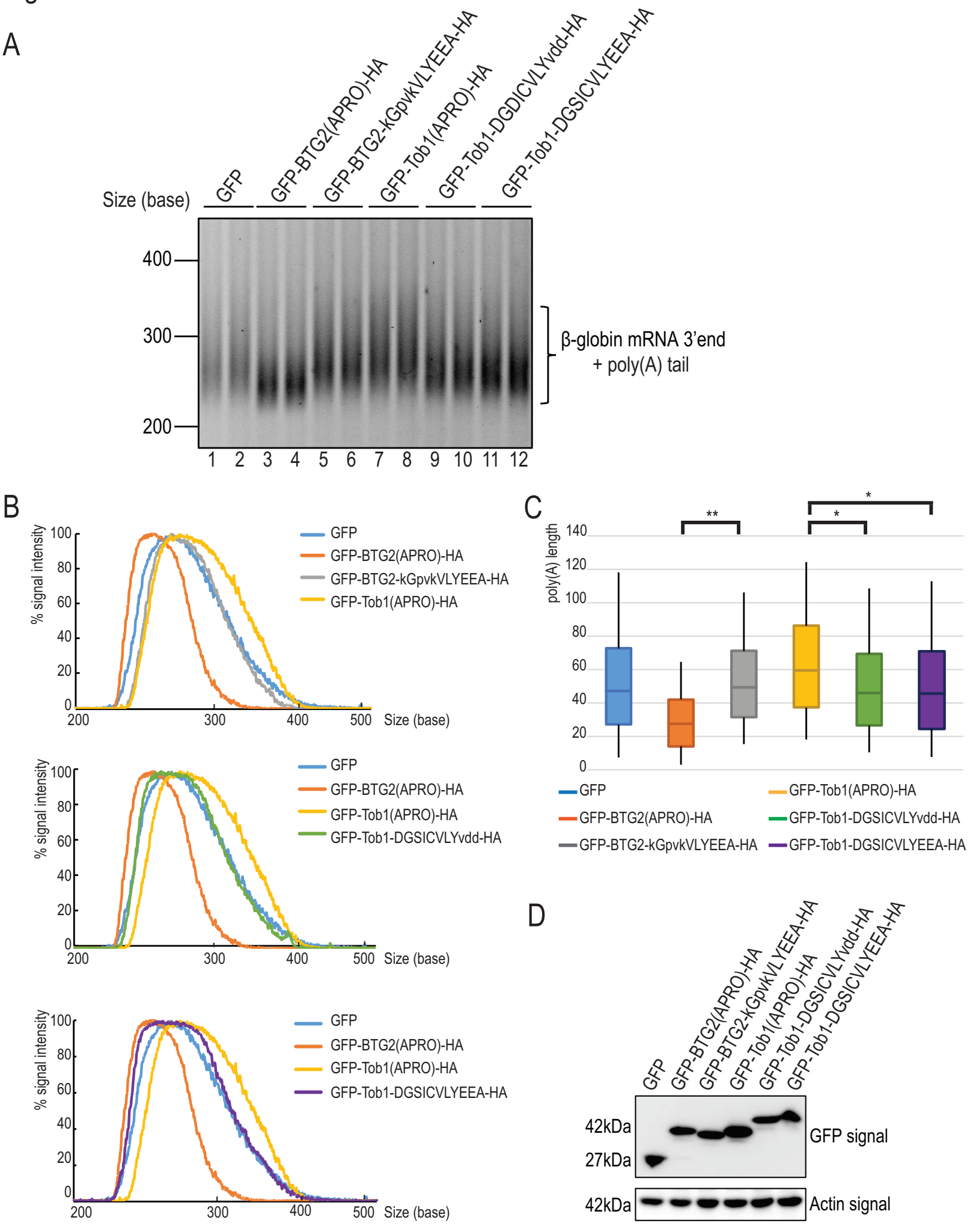

Figure 6

A

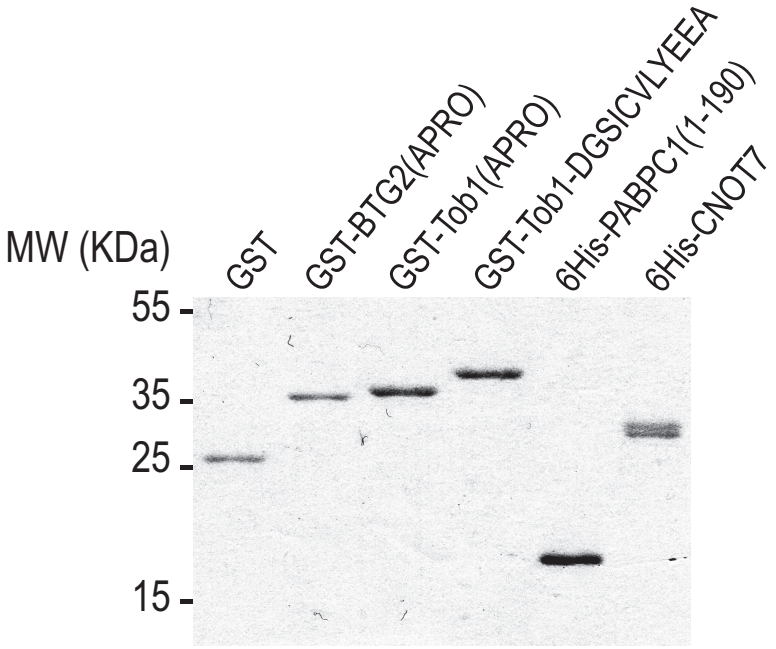
MW (KDa)
GST
GST-BTG2(APRO)
GST-Tob1(APRO)
GST-Tob1-DGSICVLYEEA
6His-PABPC1(1-190)
6His-CNOT7
55
35
25
15

B

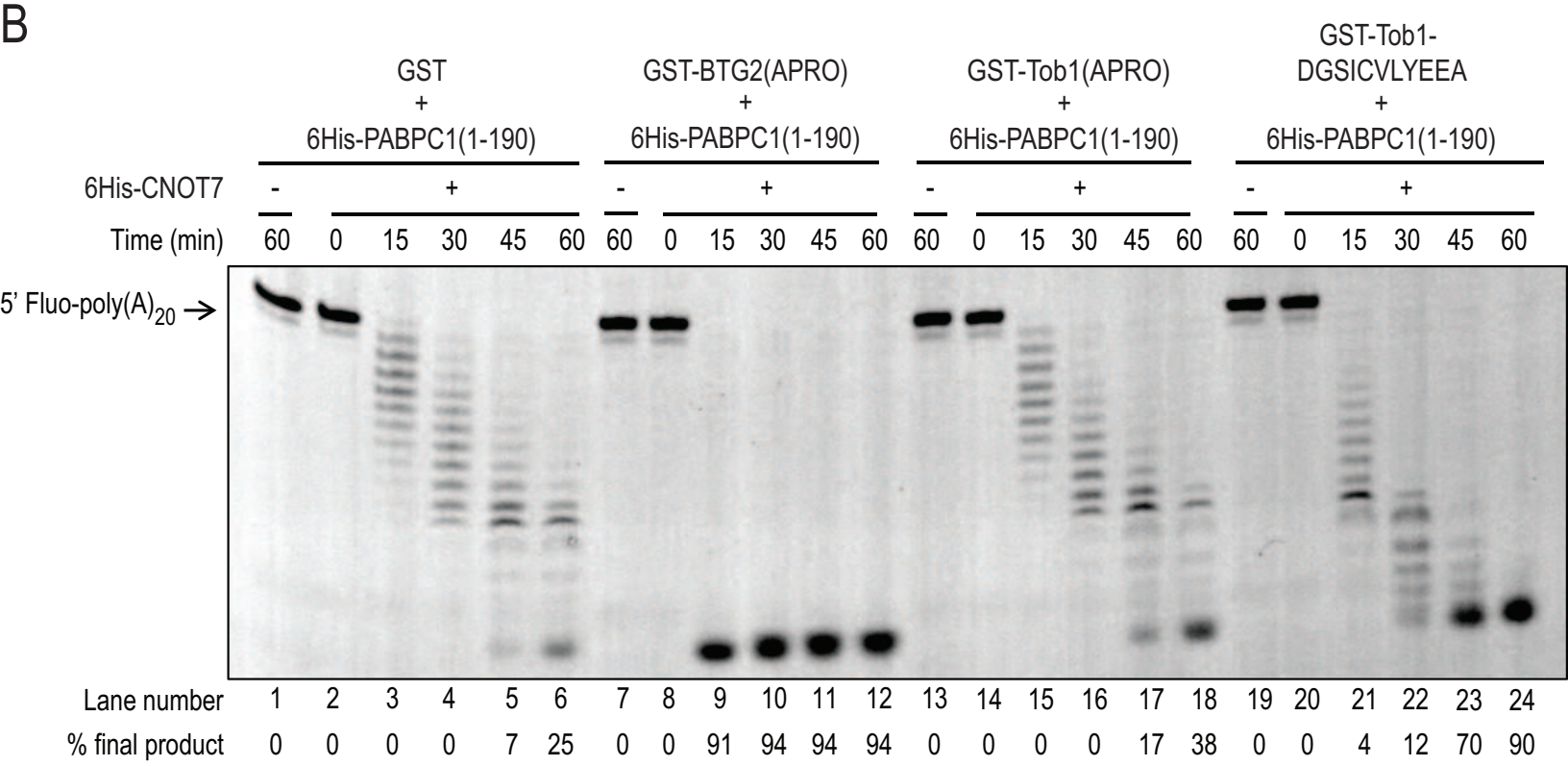
GST + 6His-PABPC1(1-190)
GST-BTG2(APRO) + 6His-PABPC1(1-190)
GST-Tob1(APRO) + 6His-PABPC1(1-190)
GST-Tob1-DGSICVLYEEA + 6His-PABPC1(1-190)
6His-CNOT7 - + - + - + - +
Time (min) 60 0 15 30 45 60 60 0 15 30 45 60 60 0 15 30 45 60 60 0 15 30 45 60
5' Fluo-poly(A)20 →
Lane number 1 2 3 4 5 6 7 8 9 10 11 12 13 14 15 16 17 18 19 20 21 22 23 24
% final product 0 0 0 0 7 25 0 0 91 94 94 94 0 0 0 0 17 38 0 0 4 12 70 90

Figure 7

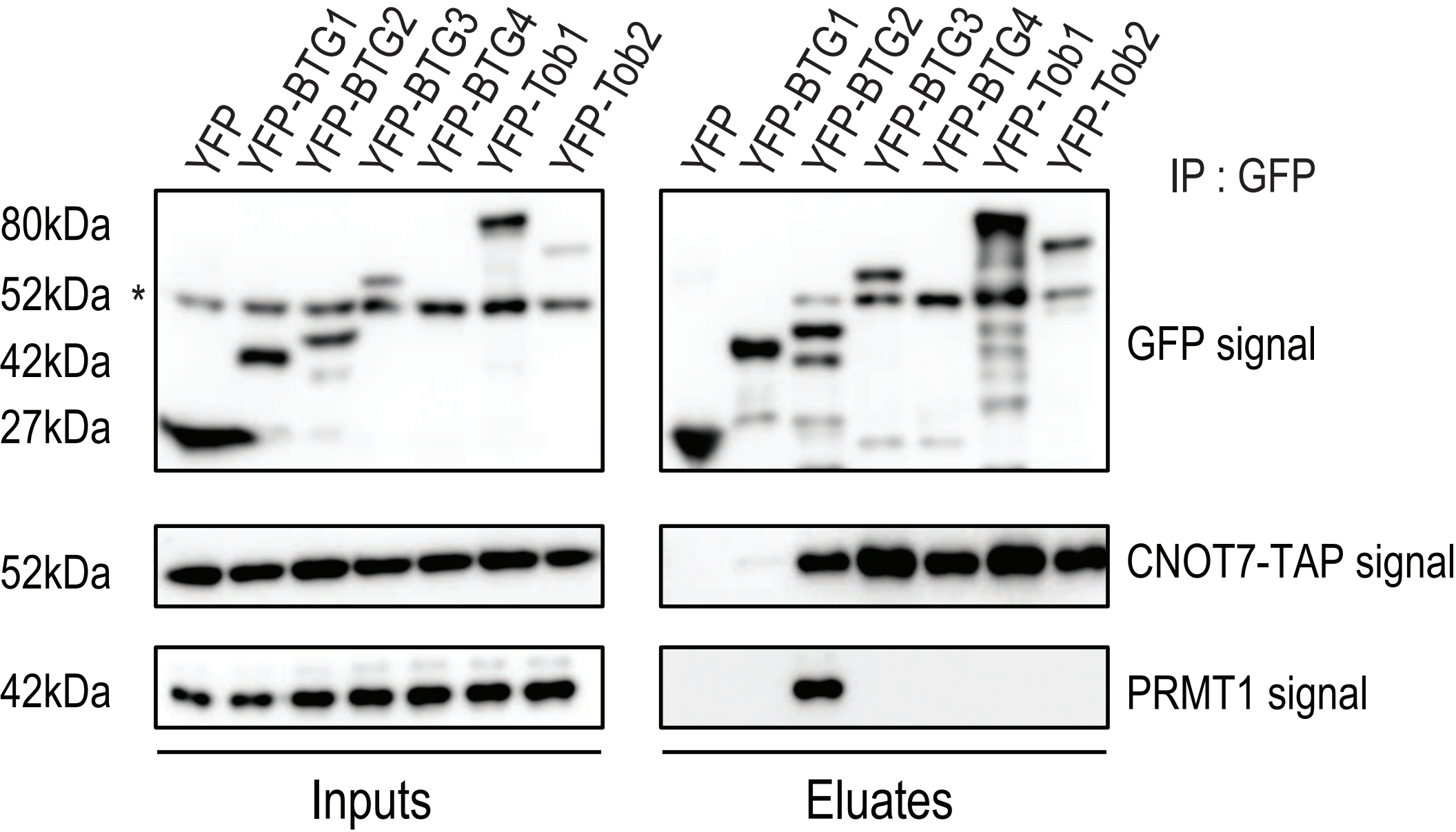

Figure 7

Figure 8

A

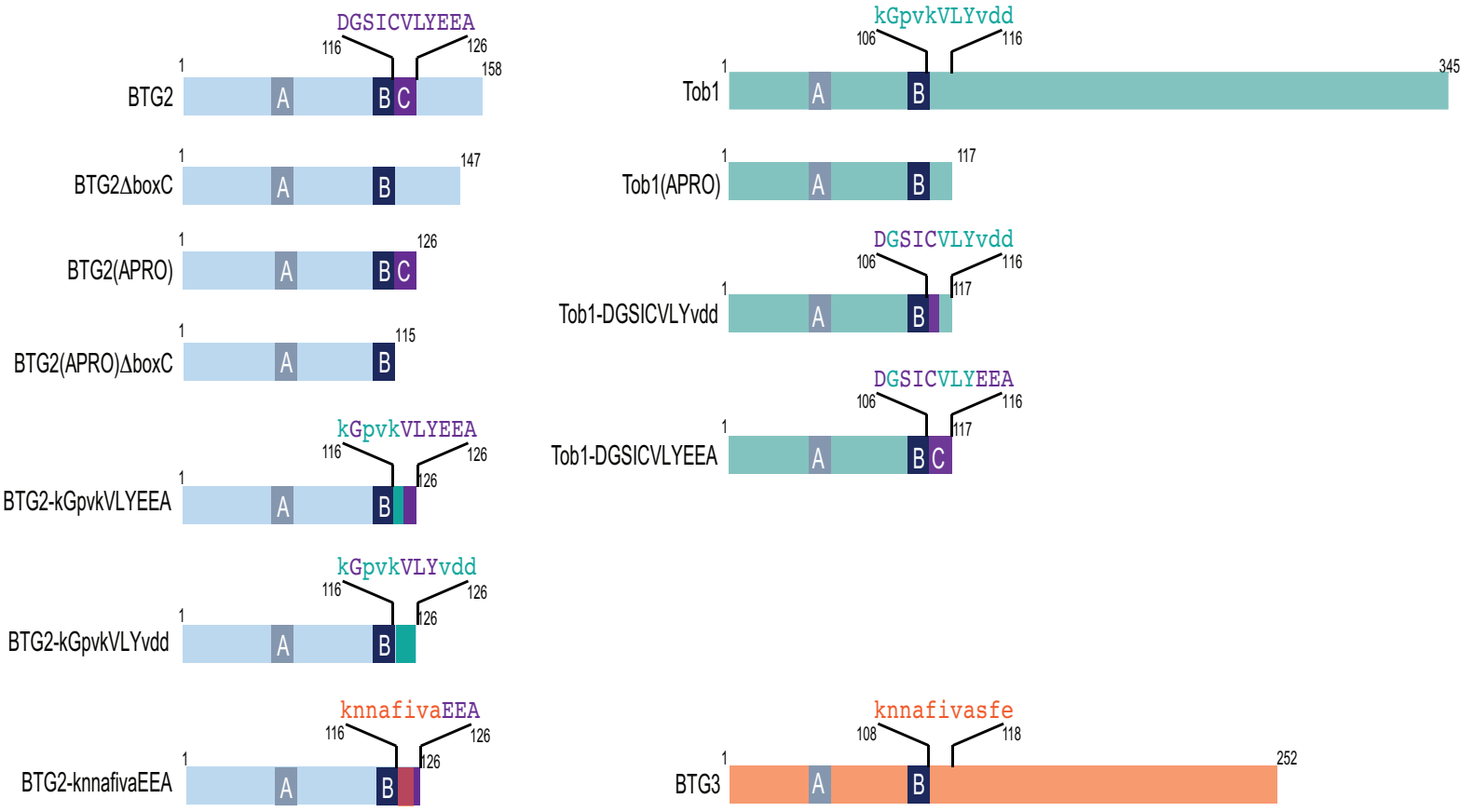
DGSICVLYEEA
116
126
1
158
BTG2
A
B C
BTG2ΔboxC
147
B
BTG2(APRO)
126
BTG2(APRO)ΔboxC
115
kGpvkVLYEEA
BTG2-kGpvkVLYEEA
kGpvkVLYvdd
BTG2-kGpvkVLYvdd
knnafivaEEA
BTG2-knnafivaEEA
kGpvkVLYvdd
106
116
Tob1
345
Tob1(APRO)
117
DGSICVLYvdd
Tob1-DGSICVLYvdd
DGSICVLYEEA
Tob1-DGSICVLYEEA
knnafivasfe
108
118
BTG3
252

B

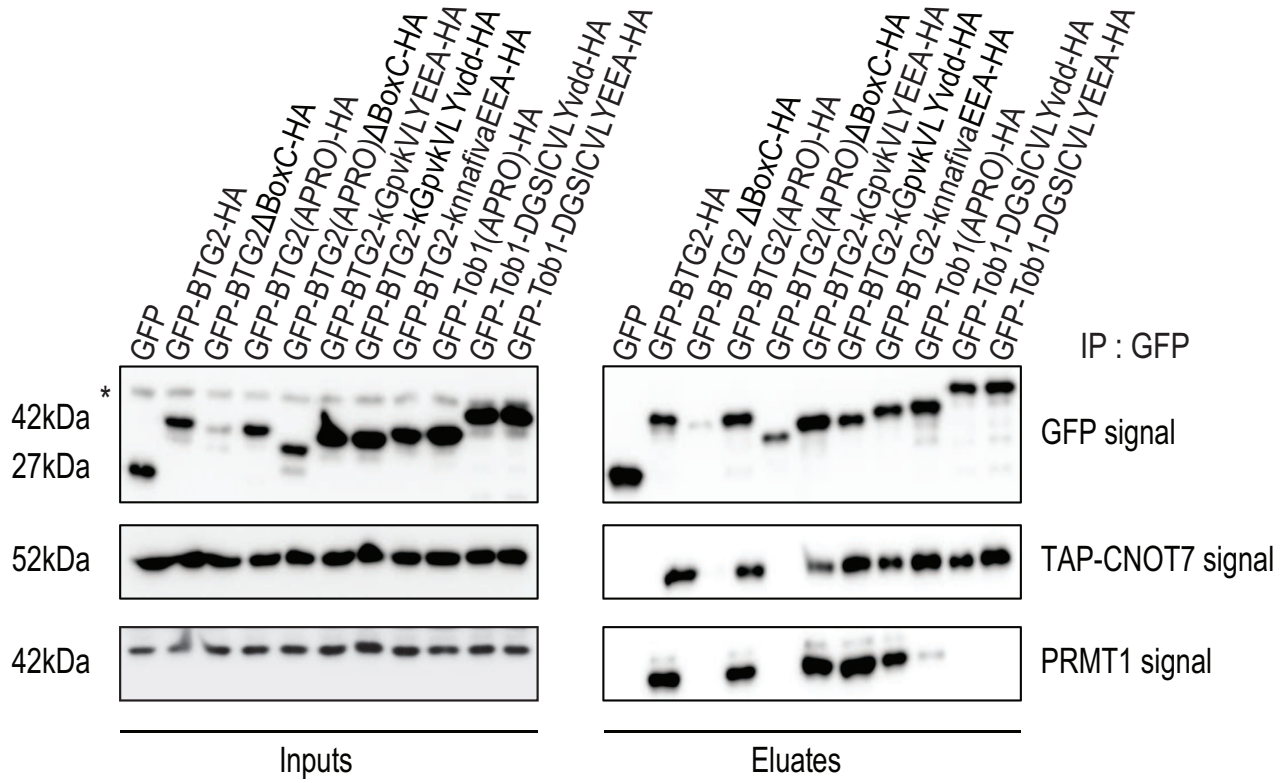
GFP
GFP-BTG2-HA
GFP-BTG2ΔBoxC-HA
GFP-BTG2(APRO)-HA
GFP-BTG2(APRO)ΔBoxC-HA
GFP-BTG2-kGpvkVLYEEA-HA
GFP-BTG2-kGpvkVLYvdd-HA
GFP-BTG2-knnafivaEEA-HA
GFP-Tob1(APRO)-HA
GFP-Tob1-DGSICVLYvdd-HA
GFP-Tob1-DGSICVLYEEA-HA
IP : GFP
42kDa
*
27kDa
GFP signal
52kDa
TAP-CNOT7 signal
42kDa
PRMT1 signal
Inputs
Eluates

Supplementary information

A conserved motif in human BTG1 and BTG2 proteins mediates interaction with the poly(A) binding protein PABPC1 to stimulate mRNA deadenylation

Hamza Amine[1-4](ORCID 0000-0001-9811-1283), Nina Ripin[5, #](ORCID 0000-0001-6099-6506), Sahil Sharma[6, §](ORCID 0000-0003-4067-5419), Georg Stoecklin[6](ORCID 0000-0001-9284-9834), Frédéric H Allain[5, 7](ORCID 0000-0002-2131-6237), Bertrand Séraphin[1-4, *](ORCID 0000-0002-5168-1921) and Fabienne Mauxion[1-4, *] (ORCID 0000-0003-0554-8211)

1 Institut de Génétique et de Biologie Moléculaire et Cellulaire (IGBMC), Illkirch, France
2 Centre National de Recherche Scientifique (CNRS) UMR 7104, Illkirch, France
3 Institut National de Santé et de Recherche Médicale (INSERM) U1258, Illkirch, France
4 Université de Strasbourg, Illkirch, France
5 Department of Biology, Institute of Molecular Biology and Biophysics, ETH Zürich, Switzerland
6 Mannheim Institute for Innate Immunoscience (MI3), Medical Faculty Mannheim, Heidelberg University, Mannheim, Germany, and Center for Molecular Biology of Heidelberg University (ZMBH), German Cancer Research Center (DKFZ)-ZMBH Alliance, Heidelberg, Germany
7 Department of Biology, Institute of Biochemistry, ETH Zürich, Switzerland

* Correspondence should be addressed to BS (seraphin@igbmc.fr) or FM (mauxion@igbmc.fr)
#: present address: Department of Chemistry and Biochemistry, University of Colorado, Boulder, CO, USA
§: present address: Institute of Molecular Infection Biology (IMIB), University of Würzburg, Germany

SUPPLEMENTARY FIGURES

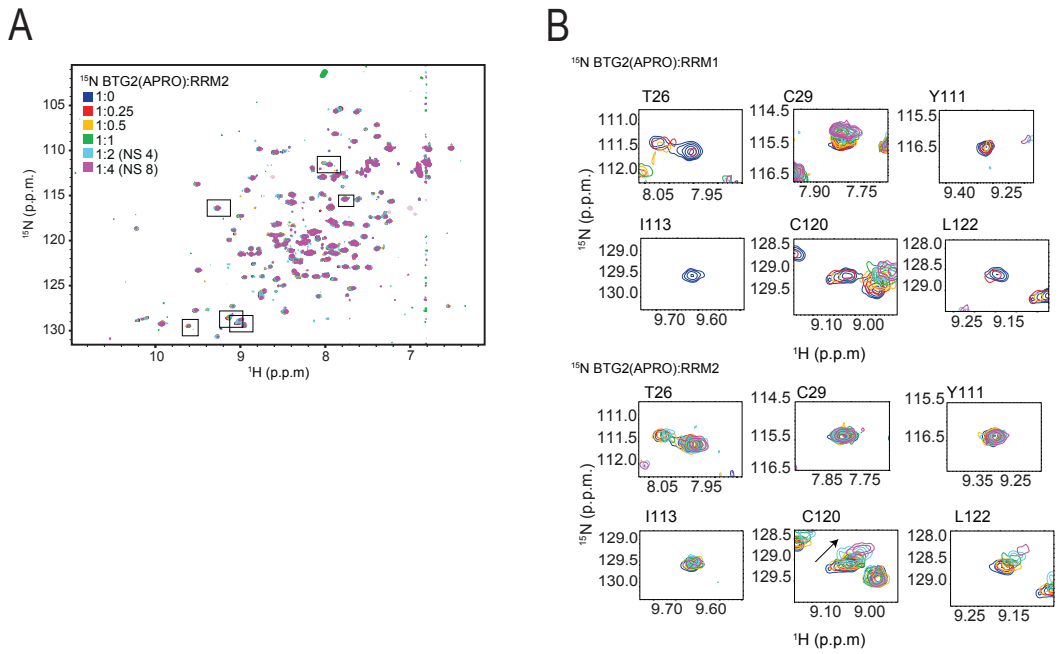

Supplemental Figure 1 - Absence or weak interaction between BTG2 and PABPC1 RRM2

A) Overlay of ^{1}H-^{15}N HSQC spectra of free BTG2(APRO) (blue) and in complex with increasing amounts of PABP RRM2 (color code as in Fig. 1A). The number of scans (NS) is 2, otherwise indicated if different.

B) Comparison of key residues of RRM1 and RRM2.

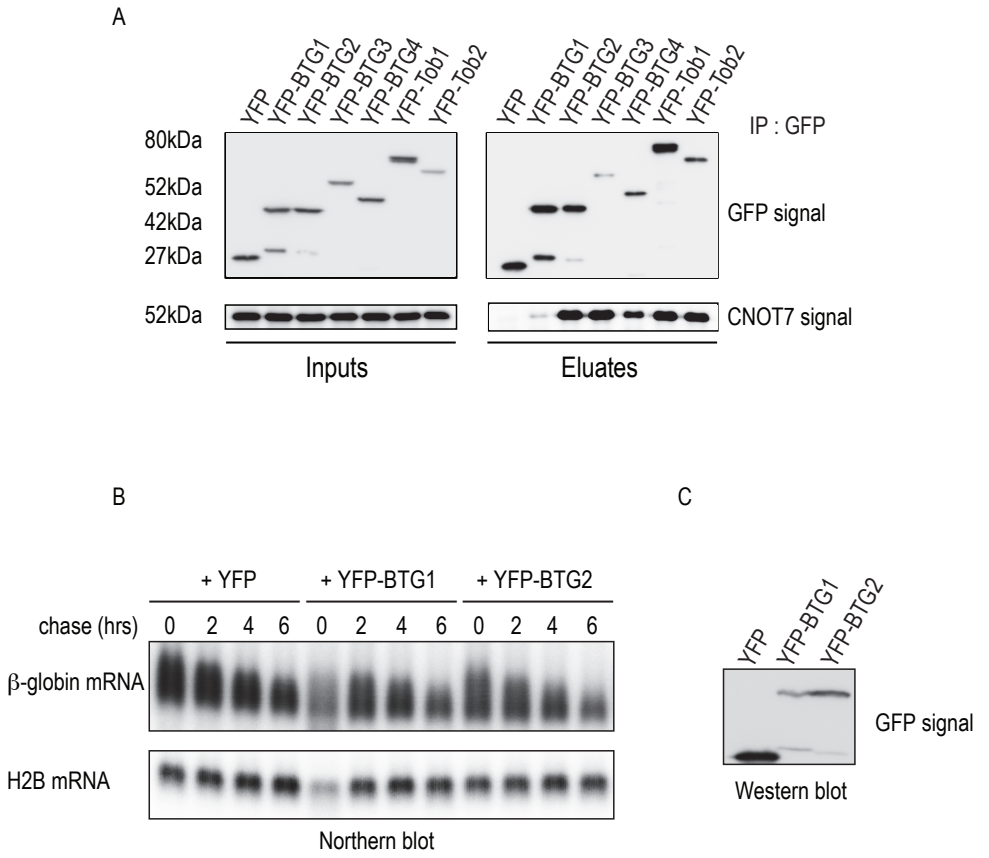

Supplemental Figure 2 - Expression of YFP-BTG1 stimulates mRNA decay despite a less efficient co-precipitation of endogenous CNOT7

A) Co-immunoprecipitation of endogenous CNOT7 with YFP-tagged BTG/Tob proteins. HEK293 cells were transfected with plasmids expressing YFP-BTG/Tob fusion proteins or only YFP as control. YFP-tagged proteins were precipitated with GFP-Trap magnetic agarose beads and the co-precipitation of endogenous CNOT7 (home-made polyclonal rabbit antiserum) was analyzed by western blotting.

B) Transcriptional chase experiments showing mRNA decay of the β-globin mRNA reporter in the presence of ectopically expressed YFP proteins. HEK293-TOF cells were co-transfected with reporter plasmid and plasmids expressing YFP-BTG1, YFP-BTG2 or YFP alone as control. Chase time indications correspond to hours after doxycyclin addition. Experiments were repeated twice. Signals obtained for replication-dependent H2B mRNAs

that are not poly-adenylated are shown as loading controls. Quantification of the results indicated half-lives of 12.25 ± 2.15, 7.7 ± 0.31 or 7.7 ± 1.53 hours respectively for the reporter co-transfected with YFP, or YFP-BTG1 or YFP-BTG2.

C) A western blot analysis of the cell lysates corresponding to the transfections performed in B is shown as a control.

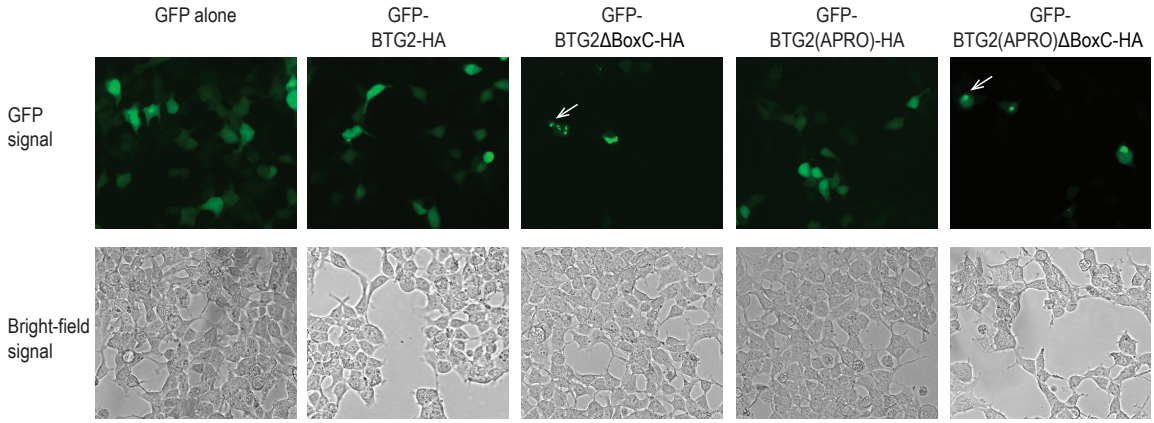

Supplemental Figure 3 - GFP-BTG2 derivatives deleted of the boxC motif accumulate in cellular aggregates

HEK293 cells were transfected with plasmids expressing GFP-BTG2 fusion derivatives or GFP alone as indicated. 24 hours after transfection, images of living cells were captured with a FLoid Cell Imaging Station (Life Technologies). Arrows point to some aggregates.

SUPPLEMENTARY TABLES

Supplementary Table 1: Plasmids used in this study

Plasmid	Vector	Insert	Reference/construction
pBS2446		cDNA human BTG2 IMAGE 5186556	
pBS2561	pET24 derivative	Encodes 6His-mouse CNOT7	Reference 1
pBS2800	pTet-ß-globin		Reference 1
pBS3352	pGEX-2T	Encodes GST-BTG2(APRO) (amino acids 1 to 126)	Reference 1
pBS3415	pET24 derivative	Encodes 6His-human PABPC1(FL)	Reference 1
pBS3425		human Tob1 cDNA	Open Biosystems clone MHS1010-7430248
pBS3426		human BTG3 cDNA	Open Biosystems clone LIFESEQ4640478
pBS3428		human BTG1 cDNA	Open Biosystems clone MHS1010-9206137
pBS3499	pCIneo	Encodes human Tob1 APRO domain (amino acids 1 to 117) with C-terminal HA tag	Reference 1
pBS3503	pGEX-2T	Encodes GST-Tob1(APRO) (amino acids 1 to 117)	Reference 1
pBS4406	pP6	Encodes a Gal4-Activating-Domain – PABPC1 (amino acids 1 to 146) fusion protein	Reference 1
pBS4409	pP6	Encodes a Gal4-Activating – Domain – human CNOT7 fusion protein	Reference 1
pBS4413	pB27	Encodes a LexA-Binding-Domain - BTG2(APRO) fusion protein	Reference 1
pBS4550	pB27	Encodes a LexA-Binding-Domain – BTG1(APRO) fusion protein	Reference 1
pBS4551	pB27	Encodes a LexA-Binding-Domain – Tob1(APRO) fusion protein	Reference 1
pBS4611	pET24 derivative	Encodes 6His-PABPC1(1-190)	Reference 1
pBS4849	pCIneo	Encodes Tob1(APRO)DGSICVLYvdd-HA	Site-directed mutagenesis of pBS3499 with OBS5628 and OBS5629 to change sequence KGPVK (amino acids 106 to 110) in Tob1 to DGSIC
pBS4944	pET24 derivative	Encodes 6HIS-PABPC1-RRM2 (amino acids 85 to 190)	PCR on pBS3415 with OBS5453+OBS6068 cut XbaI-BamHI + pET24 cut XbaI-BamHI
pBS5189	pEGFP-C3	Encodes GFP-BTG2(APRO)-HA	Reference 1
pBS5193	pEGFP-C3	Encodes GFP-BTG2(APRO)kGpvkVLYEEA-HA	Site-directed mutagenesis of pBS5189 with OBS5449 and OBS5450 to change sequence DGSIC (amino acids 116 to 120) in BTG2 to KGPVK
pBS5194	pEGFP-C3	Encodes GFP-Tob1(APRO)-HA	Reference 1
pBS5295	pEGFP-C3	Encodes GFP-BTG2-HA	Reference 1
pBS5335		human BTG4 cDNA	Dharmacon clone ID 5271706
pBS5525	pcDNA6.0	Encodes V5-His-humanTob2	This work

pBS5581	pcDNA3-YFP	Encodes YFP	
pBS5582	pcDNA3-YFP	Encodes YFP-humanBTG1(FL)	PCR on pBS3428 with G3668 and G3669 cut BglII-XhoI + pBS5581 cut BamHI-XhoI
pBS5583	pcDNA3-YFP	Encodes YFP-humanBTG3(FL)	PCR on pBS3426 with G3670 and G3671 cut EcoRI-XhoI + pBS5581 cut EcoRI-XhoI
pBS5584	pcDNA3-YFP	Encodes YFP-humanTob1(FL)	PCR on pBS3425 with G3674 and G3675 cut BglII-XhoI + pBS5581 cut BamHI-XhoI
pBS5585	pcDNA3-YFP	Encodes YFP-humanBTG2(FL)	PCR on pBS5295 with G2711 and G2752 cut BamHI-XhoI + pBS5581 cut BamHI-XhoI
pBS5586	pcDNA3-YFP	Encodes YFP-humanBTG4(FL)	PCR on pBS5335 with OBS7390+OBS7391 cut BsaI-XhoI + pBS5581 cut BamHI-XhoI
pBS5594	pcDNA3-YFP	Encodes YFP-humanTob2(FL)	PCR on pBS5525 with OBS7392+OBS7393 cut BamHI-XhoI + pBS5581 cut BamHI-XhoI
pBS5799	pCIneo	Encodes Tob1(APRO)DGSICVLYEEA-HA	Site-directed mutagenesis of pBS4849 with OBS_VDDEEA_F and OBS_VDDEEA_R to change sequence VDD (amino acids 114 to 116) in Tob1 to EEA
pBS5875	pEGFP-C3	Encodes GFP-Tob1(APRO) DGSICVLYvdd-HA	PCR cut XhoI-PstI amplified with OBS3338 and OBS6169 from pBS4849
pBS5876	pEGFP-C3	Encodes GFP-Tob1(APRO) DGSICVLYEEA-HA	PCR cut XhoI-PstI amplified with OBS3338 and OBS6169 from pBS5799
pBS5895	pB27	Encodes a LexA-Binding-Domain – Tob1(APRO) DGSICVLYvdd fusion protein	PCR cut SfiI amplified with OBS5268 and OBS8262 from pBS5875
pBS5896	pB27	Encodes a LexA-Binding-Domain – Tob1(APRO) DGSICVCLYEEA fusion protein	PCR cut SfiI amplified with OBS5268 and OBS8261 from pBS5876
pBS5903	pEGFP-C3	Encodes GFP-BTG2(APRO)DboxC	PCR cut XhoI-EcoRI amplified with OBS_deltaboxc_F and OBS_deltaboxc_R from pBS5189
pBS5915	pEGFP-C3	Encodes GFP-BTG2DboxC-HA	Site-directed mutagenesis of pBS5295 with OBS_btg2FLdeltaboxC_F and OBS_btg2FLdeltaboxC_R to delete sequence DGSICVLYEEA (amino acids 116 to 126) in BTG2
pBS5923	pEGFP-C3	Encodes GFP-BTG2(APRO) kGpvkVLYvdd-HA	Site-directed mutagenesis of pBS5189 with OBS_btg2KGPVKVLYVDD_F and OBS_btg2KGPVKVLYVDD_R to change sequence DGSICVLYEEA (amino acids 116 to 126) in BTG2 to KGPVKVLYVDD
pBS5973	pGEX-2T	Encodes GST-Tob1(APRO) DGSICVLYEEA	Site-directed mutagenesis of pBS3503 with OBS8569 and OBS8570 to to change sequence KGPVKVLYVDD to DGSICVLYEEA
pBS6111	pEGFP-C3	Encodes GFP-BTG2(APRO)knnafivaEEA-HA	Site-directed mutagenesis of pBS5189 with OBS8573 and OBS8574 to change sequence DGSICVLY (amino acids 116 to 123) in BTG2 to KNNAFIVA
pBS6163	pETGB1-1a		kind gift from G. Stier and A. Geerlof (EMBL, Heidelberg, Germany)

pBS6164	pETGB1-1a	Encodes 6His-GB1-PABPC1-RRM1 (amino acids 1 to 99)	PCR on pBS3415 with OBS1957+OBS6158 cut XhoI-BsaI + pBS6163 cut XhoI-NcoI
pBS6165	pETGB1-1a	Encodes 6His-GB1-BTG2(APRO)	PCR on pBS5295 with OBS668+OBS6726 cut EcoRI-BspHI + pBS6163 cut NcoI-EcoRI
pBS6166	pETGB1-1a	Encodes 6His-GB1-BTG2(APRO)kGpvkVLYEEA	PCR on pBS5193 with OBS668+OBS7487 cut EcoRI-BspHI + pBS6163 cut NcoI-EcoRI
pBS6167	pETGB1-1a	Encodes 6His-GB1-BTG2	PCR on pBS2446 with OBS668+OBS2316 cut EcoRI-BspHI + pBS6163 cut NcoI-EcoRI

Supplementary Table 2: Oligonucleotides used in this study

Name	**Sequence**
G2711	ATTGGATCCATGAGCCACGGGAAGG
G2752	GGCCTCGAGGCTGGAGACTGCCATCAC
G3668	ATATAGATCTATGCATCCCTTCTACACC
G3669	ATATCTCGAGTTAACCTGATACAGTCAT
G3670	ATATGAATTCATGAAGAATGAAATTGCT
G3671	ATATCTCGAGTTAGTGAGGTGCTAACAT
G3674	ATATAGATCTATGCAGCTTGAAATCCAA
G3675	ATATCTCGAGTTAGTTAGCCATAACAGG
OBS_btg2FLdeltaboxC_F	GCGGCCAGTGGGCCTCCCCAATGC
OBS_btg2FLdeltaboxC_R	GCATTGGGGAGGCCCACTGGCCGC
OBS_btg2KGPVKVLYVDD_F	CAAGGTCTTGTACGTGGACGACAATATGTACCCATAACGAC
OBS_btg2KGPVKVLYVDD_R	GTCGTATGGGTACATATTGTCGTCCCAACGTACAAGACCTTGA
OBS_deltaboxc_F	CCGCTCGAGACCATGAGCCACGGGAAGGGAA
OBS_deltaboxc_R	TATGAATTCTTACTCCCCAATGCGGTAGGA
OBS_VDDEEA_F	GGATCCATCTGCGTGCTTTACGAGGAGGCGAATTCCATGTACCC
OBS_VDDEEA_R	CCTAGGTAGACGCACGAAATGCTCCTCCGCTTAAGGTAGATGGG
OBS668	GGATGCGGCCGCAATCATGAGCCACGGGAAGGGAACCGA
OBS1957	GCGCTCATGAACCCCAGTGCCCCCAG

OBS2316	CGGGAATTCTAGCTGGAGACTGCCATCAC
OBS3338	GGCCTCGAGGGATCCATGCAGCTTGAAATCCAAGTAG
OBS5268	ATCGGCCGGACGGGCCATGCAGCTTGAAATCCAAGTAG
OBS5449	CCGCATTGGGGAGAAGGGCCCCGTCAAGGTCTTGTACGAGGAGGC
OBS5450	GCCTCCTCGTACAAGACCTTGACGGGGCCCTTCTCCCCAATGCGG
OBS5453	GCCGGATCCTTAGAATTCTTTTGCCCTAGCTCCAAGTTC
OBS5628	CCAAATTGGTGAAGACGGATCCATCTGCGTGCTTTACGTGGATG
OBS5629	CATCCACGTAAAGCACGCAGATGGATCCGTCTTCACCAATTTGG
OBS6068	GGCTCTAGATAAGGAGGATATATATGCATCACCATCACCATCACATGTGGTCTCAGCGTGATCCA
OBS6158	GCCCTCGAGTTAGCCTACTCCACTTTTGCGAAG
OBS6169	GACCTGCAGTCATGCGTAGTCTGGTACGTCGTAT
OBS6726	ACCGAATTCCTAGGCCTCCTCGTACAAGACGC
OBS7381	CTGGGATCCTTATGGCGACTGTCGAACC
OBS7390	AACGGTCTCGGATCCATGAGAGATGAAATTGCAACAA
OBS7392	TCAGGATCCATGCAGCTAGAGATCAAAGTGGC
OBS7393	AACCTCGAGTCAGTTGGCCAGCACCACGG
OBS7487	ACCGAATTCCTAGGCCTCCTCGTACAAGACCTT
OBS8261	ATCGGCCCCAGTGGCCCTTAATTCGCCTCCTCGTAAAGCACG
OBS8262	ATCGGCCCCAGTGGCCCTTAATTATCATCCACGTAAAGCACG
OBS8569	GTTTCTTACCAAATTGGTGAAGACGGCTCCATCTGCGTCTTGTACGAGGAGGCCAATTAGAATTCATCGTGACTG
OBS8570	CAGTCACGATGAATTCTAATTGGCCTCCTCGTACAAGACGCAGATGGAGCCGTCTTCACCAATTTGGTAAGAAAC
OBS8573	TCCTACCGCATTGGGGAGAAAAACAATGCATTCATTGTTGCC

	GAGGAGGCCAACATGTA
OBS8574	TACATGTTGGCCTCCTCGGCAACAATGAATGCATTGTTTTTCT CCCCAATGCGGTAGGA

SUPPLEMENTARY METHODS

Transcriptional chase experiments and Northern blot analysis

HEK293 Tet-Off cells were transfected with 0.4 μg of the pTet-β-globin plasmid (pBS2800) and 0.4 μg of the GFP-BTG expressing plasmids in 6-cm diameter culture dishes with Effectene transfection reagent (Qiagen). Two days after transfection, a transcriptional chase was performed by addition of doxycyclin (2 μg/ml). Chase times correspond to hours after doxycyclin addition and to times of RNA extraction.

10 μg of total RNA was electrophoresed onto 1.4% agarose/6% formaldehyde gels and transferred to Hybond-N+ membranes (GE Healthcare). After transfer, blots were stained with methylene blue to check for equal loading and hybridized to probes synthesized by in vitro transcription with the T7 RNA polymerase (Promega). Hybridization signals were visualized with Typhoon FLA 9500 (GE Healthcare).

SUPPLEMENTARY REFERENCES

1. Stupfler B, Birck C, Seraphin B, Mauxion F. BTG2 bridges PABPC1 RNA-binding domains and CAF1 deadenylase to control cell proliferation. Nature communications 2016; 7:10811.